Volume 54(7): 773–780, 2006
Journal of Histochemistry & Cytochemistry
http://www.jhc.org

ARTICLE

Improved RT-PCR Amplification for Molecular Analyses with Long-term Preserved Formalin-fixed, Paraffin-embedded Tissue Specimens

Kiyohiro Hamatani, Hidetaka Eguchi, Keiko Takahashi, Kazuaki Koyama, Mayumi Mukai, Reiko Ito, Masataka Taga, Wataru Yasui, and Kei Nakachi

Department of Radiobiology/Molecular Epidemiology, Radiation Effects Research Foundation, Hiroshima, Japan (KH,HE,KT,KK,MM,RI,MT,KN), and Hiroshima University Graduate School of Biomedical Sciences, Hiroshima, Japan (WY)

SUMMARY Recently, in addition to DNA, RNA extracted from archival tissue specimens has become an invaluable source of material for molecular biological analysis. Successful amplification with PCR/RT-PCR is problematic when using amplicons of short size due to degradation of DNA or RNA. We established an improved method for efficient RT-PCR amplification of RNA extracted from archival formalin-fixed, paraffin-embedded tissue by the elimination of RNA modification and the restoration of RNA template activity. Namely, the preheating in citrate buffer (pH 4.0) of RNA extracted from long-term preserved tissue specimens resulted in significantly increased efficiency of RT-PCR. (J Histochem Cytochem 54:773–780, 2006)

KEY WORDS
preheating of RNA
archival formalin-fixed and paraffin-embedded tissue
citrate buffer
modification of RNA by formalin
RT-PCR amplification

RETROSPECTIVE ANALYSIS of archival tissue specimens is indispensable especially for studies of rare cancers or cancers associated with exposure to uncommon past events such as Thorotrast treatment, nuclear power station accidents, or atomic bombings. In recent years, application of new molecular techniques including polymerase chain reaction (PCR) to analysis of archival tissue samples is anticipated to bring about better understanding of the molecular mechanisms of these cancers (Mies 1994). However, most surgical and autopsy tissue specimens have been preserved as formalin-fixed and paraffin-embedded blocks for long periods of time: DNA or RNA is often found to degrade under such conditions.

Extraction of DNA from formalin-fixed, paraffin-embedded tissue for PCR analysis has been well documented (Jackson et al. 1990; Forsthoefel et al. 1992; Frank et al. 1996). On the other hand, RNA was first extracted from formalin-fixed, paraffin-embedded tissue for Northern and dot-blotting analysis (Rupp and Locker 1988). Subsequently, many reports were made about extraction of viral or human cellular RNA from archival samples and successful amplification of extracted RNA (Weizäcker et al. 1991; Bresters et al. 1992; Finke et al. 1993; Koopmans et al. 1993; Goldsworthy et al. 1999; Masuda et al. 1999; Körbler et al. 2003; Byers et al. 2004). Recent reports showed that RNA extracted from formalin-fixed, paraffin-embedded tissue samples was also available for quantitative analyses of gene expression (Lehmann and Kreipe 2001; Specht et al. 2001; Cohen et al. 2002; Kim et al. 2003; Cronin et al. 2004).

Nevertheless, persistent demands have been made for further improvement in RNA extraction from long-term preserved tissue samples whose RNA significantly degraded being chemically modified. The problems facing this goal include degradation of RNA in tissue due to delay before fixation, prolonged fixation, or long-term preservation after fixation (Bresters et al. 1994; Cronin et al. 2004), low efficiency of RNA extraction because of cross-linking with proteins (Finke et al. 1993; Park et al. 1996), and impaired reverse transcriptase reaction (Masuda et al. 1999) by formalin-induced modification (addition of mono-methylol to amino groups of four bases) of extracted RNA (Feldman 1973; Auerbach et al. 1977; Masuda et al. 1999). To overcome this problem, heat treatment of RNA prior to reverse transcription has been proposed. For example, it was reported that the chemical modification of all four bases of RNA by fixation in phosphate-buffered

Correspondence to: Kiyohiro Hamatani, Department of Radiobiology/Molecular Epidemiology, Radiation Effects Research Foundation, 5-2 Hijiyama Park, Minami-ku, Hiroshima-shi, Hiroshima 732-0815, Japan. E-mail: hamatani@rerf.or.jp

Received for publication October 19, 2005; accepted February 14, 2006 [DOI: 10.1369/jhc.5A6859.2006].

0022-1554/06/$3.30

formalin can be reversed to some extent by incubation in TE buffer (pH 7.0) at 70C for 1 hr, resulting in restoration of template activity of RNA in RT-PCR (Masuda et al. 1999).

While performing molecular analyses on cancer tissue specimens taken from atomic bomb survivors and that were stored for several decades (up to 50 years), we frequently encountered archival unbuffered formalin-fixed, paraffin-embedded specimens that were difficult to use for RT-PCR analysis. We found that significant degradation and chemical modification of RNA greatly affected RT-PCR amplification.

Removal of chemical modification from bases of RNA as well as significant reduction of amplicon size may be crucial for the enhanced availability of limited archival unbuffered formalin-fixed, paraffin-embedded tissue samples. Therefore, we examined whether the preheating of RNA extracted from archival unbuffered formalin-fixed, paraffin-embedded tissues enhances the efficiency of RT-PCR, along with determining optimal conditions for the RNA preheating. Application of this preheating technique to retrospective research is expected to enhance the availability of archival unbuffered formalin-fixed, paraffin-embedded tissue specimens for molecular analysis that have been stored for several decades and have functioned as a source for histological evaluation, to allow better understanding of molecular characteristics of various diseases.

Materials and Methods

Tissue

Five archival unbuffered formalin-fixed, paraffin-embedded thyroid cancer tissue samples for in-house control were used in this study. All samples were preserved at room temperature for 19 to 21 years. After deparaffinization of 5-μm sections by Hemo-De (Fujisawa Yakuhin Kogyo; Osaka, Japan) and staining with methylgreen (Sigma-Aldrich; St. Louis, MO), cancerous regions (~2–3 × 3 mm) were isolated using a laser microdissection system (Leica AS LMD; Wetzlar, Germany). All cancerous regions microdissected from six to eight successive tissue sections were combined for RNA extraction.

RNA Extraction and Measurement

RNA was isolated from microdissected tissue using the High Pure RNA Paraffin Kit according to the manufacturers instructions (Roche Diagnostics; Basel, Switzerland), with some modifications. Briefly, microdissected tissue was digested with proteinase K at 55C overnight, followed by DNase I treatment. After the lysate was purified by High Pure filter, RNA was eluted twice with 100 μl of RNase-free water. RNA was then precipitated by ethanol in the presence of 2 μl of ethachinmate (Nippon Gene; Tokyo, Japan) as a carrier and resuspended in 30 μl of RNase-free water. The concentration of RNA was measured by absorption at 260 nm with a spectrophotometer (Gene Spec III; Hitachi, Tokyo, Japan). The quality of extracted RNA was measured by electrophoresis on 1.5% or 3.0% native agarose gel and 2.5% formaldehyde agarose gel.

Heat Treatment of RNA

Approximately 150 ng of total RNA was heated in 250 μl of 10 mM citrate buffer with various pH values ranging from 3 to 6.5 at 70C for a number of different time periods. Preheating in 250 μl of 10 mM sodium borate with various pH values (pH 6.5–10) or 10 mM TE buffer (pH 7.0, 7.5, and 8.0) was similarly carried out. After preheating, RNA was precipitated by ethanol in the presence of ethachinmate as carrier and dissolved in RNase-free water to arrive at a final concentration of 10 ng/μl.

cDNA Synthesis

One hundred ng of total RNA and 50 pmol/μl of random primers (9 mer) were heated in 11 μl of RNase-free water at 65C for 10 min and chilled in ice water. A mixture consisting of 4 μl of 5× RT buffer, 2 μl of 20 mM DTT, 1 μl of 10 mM dNTPs, and 1 μl of RNase Inhibitor (20 U/μl; Takara, Tokyo, Japan) was added to RNA solution and incubated at room temperature for 5 min. After addition of 1 μl of ReverTra Ace (100 U/μl; Toyobo, Osaka, Japan), a reaction mixture was incubated at 42C for 60 min and at 70C for 15 min.

Detection of Expression of Breakpoint Cluster Region (*BCR*) and *N-ras* Genes by RT-PCR

RT-PCR was performed in a 25-μl volume containing 1× PCR buffer, 200 μM each of dATP, dCTP, dGTP, and dTTP, 1.5–3.0 mM $MgCl_2$, 0.4 μM of each specific primer, 0.5 U Platinum Taq DNA polymerase (Invitrogen; Carlsbad, CA), and 2 μl of cDNA from the previous RT reaction. Primary denaturation

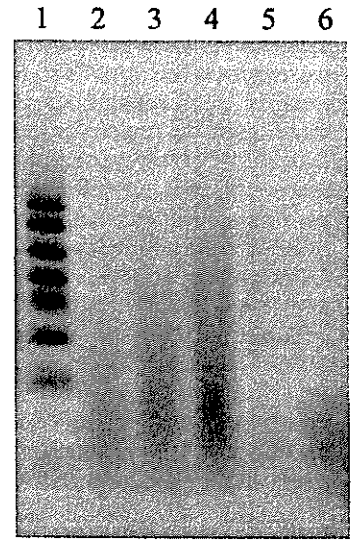

Figure 1 Total RNA extracted from archival unbuffered formalin-fixed, paraffin-embedded thyroid cancer tissue. The extracted RNA was electrophoresed on 3% native agarose gel. Lanes 2–4 contain RNA from three different archival samples. Lane 1, 100-nucleotide RNA marker; Lanes 5 and 6, 70 base-synthesized nucleotides (25 ng and 100 ng/lane, respectively).

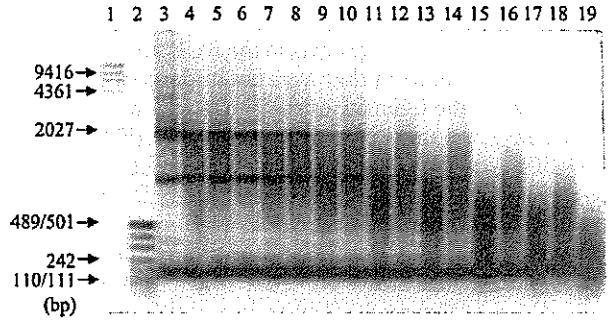

Figure 2 Effect of preheating temperature on RNA integrity. Two μg of total RNA extracted from frozen human thyroid cancer cell line were heated for 15 min or 30 min at various temperatures (Lanes 4 and 5, 60C; Lanes 6 and 7, 65C; Lanes 8 and 9, 70C; Lanes 10 and 11, 75C; Lanes 12 and 13, 80C; Lanes 14 and 15, 85C; Lanes 16 and 17, 90C; Lanes 18 and 19, 95C). Lane 3, no heating; Lane 1, λ HindIII DNA marker; Lane 2, pUC19-MspI digest for DNA size marker. Electrophoresis was done on 1.5% native agarose gel. Fifteen min heating is for Lanes 4, 6, 8, 10, 12, 14, 16, and 18. Thirty min heating is for Lanes 5, 7, 9, 11, 13, 15, 17, and 19.

(95C for 3 min) and final extension (72C for 5 min) were the same for each RT-PCR reaction, all of which were subjected to 40 cycles of amplification consisting of 95C for 30 sec, 55–60C for 30 sec and 72C for 30–45 sec for *BCR*, and 95C for 30 sec, 52–55C for 30 sec and 72C for 30–45 sec for *N-ras*. For positive and negative controls of RT-PCR, cDNA derived from human thyroid cancer cell line (8505C) and H_2O were used as templates, respectively. Five μl of the reaction mixture was run on an 8% acrylamide gel and visualized with ethidium bromide. In each experiment, it was confirmed that all target bands were the real ones by digestion of restriction enzyme, which existed within each amplified target fragment. Since all the primer sets used were designed to locate in two different exons, no amplification of RNA without RT was observed. The effects of preheating on RT-PCR efficiency were examined by amplifying the fragments of different sizes in the *BCR* gene (eight different sizes: 61 bp, 94 bp, 127 bp, 152 bp, 175 bp, 222 bp, 250 bp, and 275 bp) and the *N-ras* gene (seven different sizes: 61 bp, 98 bp, 121 bp, 148 bp, 199 bp, 221 bp, and 250 bp). The semiquantification of each PCR product was made by measurement of the intensity of each band using Kodak (Tokyo, Japan) 1D Image Analysis Software.

Results

RNA Extracted from Unbuffered Formalin-fixed, Paraffin-embedded Tissue

We extracted RNA from five different archival unbuffered formalin-fixed, paraffin-embedded thyroid cancer tissue specimens, as described in Materials and Methods. An image of electrophoresis of these RNA is shown in Figure 1. They appeared as smears on agarose gel with no ribosomal bands observed in any of the samples. The range of smeared RNA differed slightly

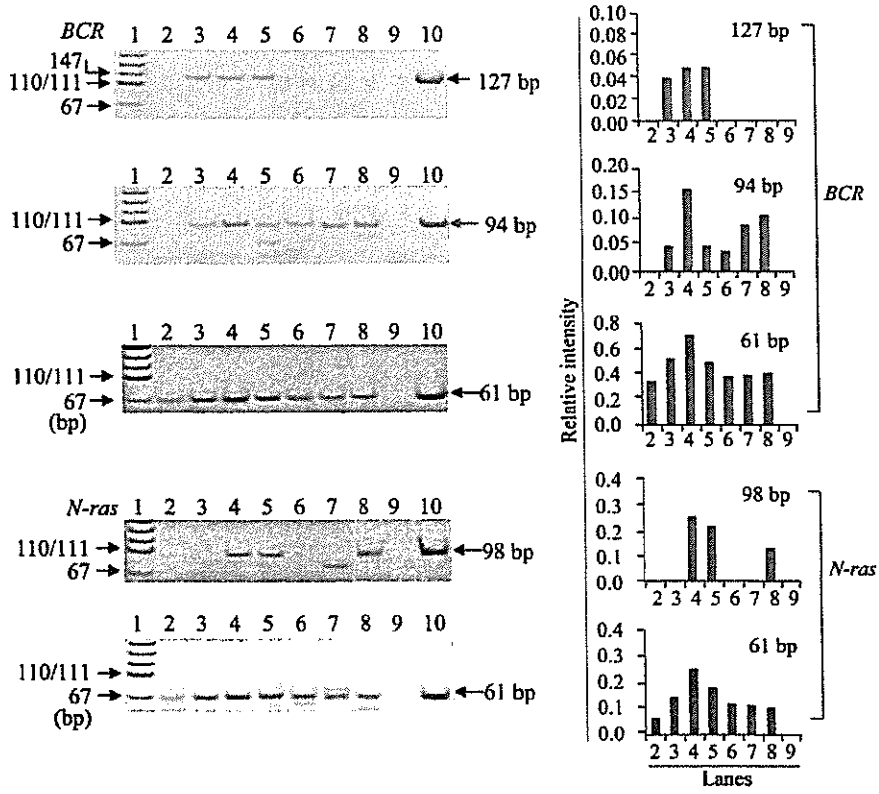

Figure 3 Effect of pH on RT-PCR amplification of RNA. Efficiency of RT-PCR amplification of RNA preheated at 70C for 30 min in various pHs (Lane 3, pH 3.0; Lane 4, pH 4.0; Lane 5, pH 5.0; Lane 6, pH 6.0; Lane 7, pH 6.5) was measured by amplifying 61-, 94-, and 127-bp fragments in the *BCR* gene and 61- and 98-bp fragments in the *N-ras* gene. Lane 2, no preheating; Lane 8, preheated with TE (pH 7.0) for 30 min; Lane 9, negative control; Lane 10, positive control; Lane 1, pUC19-MspI digest for DNA size marker. The bands different from the position shown by arrow indicate the extra bands. This is the same in Figures 2–5. Bar graphs at right indicate the relative intensity of each target band when intensity of positive control is assumed to be 1.0. The numbers on the horizontal axis correspond to the number of lanes in the left electrophoresis. This labeling is also used in Figures 3–5.

among five archival tissue specimens. A majority of the smeared RNA sample used for determination of the conditions for preheating of RNA ranged from ~70 to 100 bases (Figure 1, Lane 2). Other RNA samples showing better efficiency of RT-PCR amplification than the previous one ranged from ~70 to 200–300 bases (Figure 1, Lanes 3 and 4). The size of RNA from the remaining two tissue samples was the intermediate among the other three samples.

Temperature in Preheating of RNA

At first we tested the effects of incubation at different temperatures on RNA stability using intact RNA prepared from human thyroid cancer cell lines, because it is hard to evaluate the preheating effect using already degraded RNA extracted from formalin-fixed, paraffin-embedded tissue specimens (Figure 2). Preheating of RNA at >80C for 30 min in H_2O resulted in vigorous degradation. Considering our result and a report by Masuda et al. (1999), we set preheating temperature at 70C in this study.

Effects of pH in Preheating of RNA on RT-PCR Amplification

Using the RNA with the worst efficiency of RT-PCR amplification among the five archival tissue samples, we examined the effects of preheating on RT-PCR efficiency by amplifying the fragments of different sizes in the *BCR* gene and the *N-ras* gene (Figure 3). There were 61-bp fragments in the *BCR* and *N-ras* genes detected in the RNA that were not undergoing preheating, although the intensity of the bands was weak compared with that in the RNA with preheating (Figure 3). Preheating of RNA in 10 mM citrate buffer at pH 3–5 at 70C for 30 min made amplification of 94- and 127-bp fragments possible in the *BCR* gene and 98-bp fragments in the *N-ras* gene. These same fragments could not be amplified by RT-PCR without undergoing preheating (Figure 3). Preheating of RNA in citrate buffer with pH ~4 was the most effective method in the RT-PCR amplification of the *BCR* and *N-ras* genes. To determine optimal pH, we further investigated in detail the effects of pH on RT-PCR amplification using preheated RNA. As shown in Figure 4, RNA treated with ~pH 4.0 showed the most efficient RT-PCR amplification of both the *BCR* and *N-ras* genes among citrate buffers with different pH values ranging from 3 to 5 and TE (pH 7.0). We also examined the effect of pH range (6.5–10) on RT-PCR amplification using 10 mM sodium borate solution and TE. Among buffers ranging from pH 7.0 to pH 8.0 (TE buffers with pH 7.0, 7.5, and 8.0 and borate buffer with 8.0), little difference was found in the effect of preheating with these buffers at a concentration of 10 mM (data not shown). The effect of preheating decreased with increased pH, and adverse effect was observed in RNA treated with pH 9.0 or 10.0 (data not

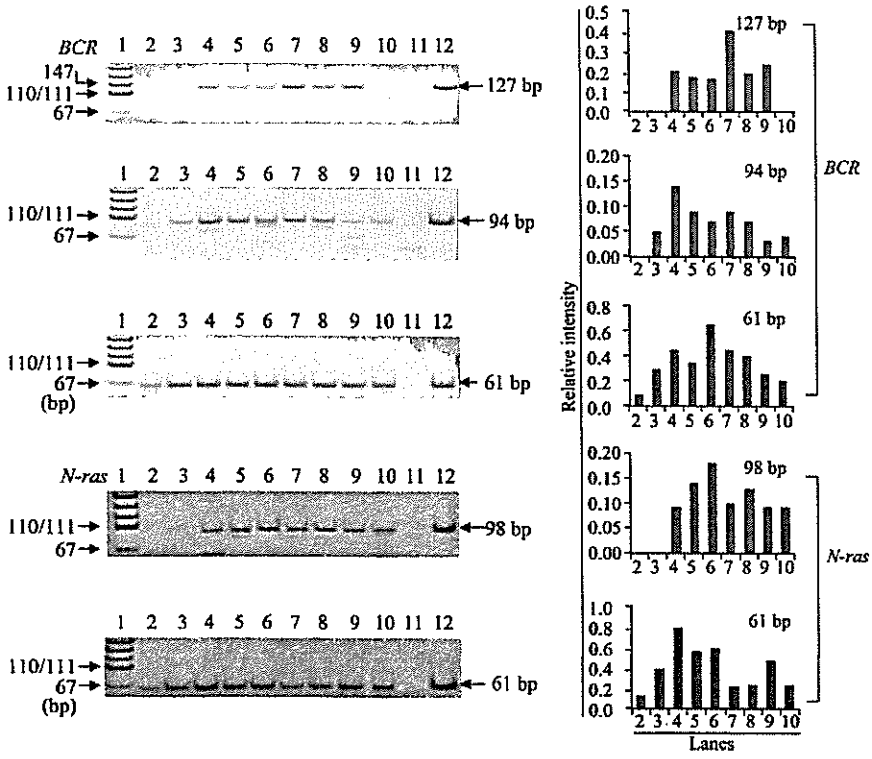

Figure 4 Detailed analysis of pH of citrate buffer ranging from 3.0 to 5.0 for optimization of preheating condition. RNA was preheated in citrate buffer (Lane 3, pH 3.0; Lane 4, pH 3.5; Lane 5, pH 3.7; Lane 6, pH 4.0; Lane 7, pH 4.25; Lane 8, pH 4.5; Lane 9, pH 5.0) at 70C for 30 min before cDNA was synthesized. RT-PCR amplification of *BCR* and *N-ras* mRNAs was carried out to determine the optimal pH for preheating of RNA. Lane 2, no preheating; Lane 10, preheated with TE (pH 7.0) for 30 min; Lane 11, negative control; Lane 12, positive control; Lane 1, pUC19-MspI digest for DNA size marker.

shown). Little difference was found in efficiency of RT-PCR amplification enhanced by preheating of RNA between citrate buffer (pH 6.5) and sodium borate (pH 6.5) (data not shown).

Effects of Buffer Concentration in Preheating of RNA on RT-PCR Amplification

We examined the effects of different buffer concentrations on RT-PCR amplification. In both *BCR* and *N-ras* target genes, when RNA was heated with 50 mM citrate buffer at 70C, even 61-bp fragments were hard to detect. There was a lower efficiency of RT-PCR amplification than amplification without preheating (Figure 5). On the other hand, treatment with 10 mM citrate buffer resulted in the greatest efficiency of RT-PCR amplification among concentrations investigated (Figure 5).

Effects of Preheating Time of RNA on RT-PCR Amplification

We examined the effects of preheating time on RT-PCR amplification. As shown in Figure 6, preheating in citrate buffer (pH 4.0) at 70C for 45 min was the most effective method for RT-PCR amplification. Thus, the efficiency of RT-PCR amplification depends on pH, concentration of buffer, and incubation time. In the other four archival thyroid tissue samples, we also examined whether preheating of RNA in citrate buffer (pH 4.0) at 70C for 45 min resulted in enhanced efficiency of RT-PCR amplification. We found that the longer fragments in the preheated RNA could be amplified in all cases compared with the non-treated RNA, although the amplified fragment sizes differed among these thyroid tissue samples (Figure 7). Increased efficiency of RT-PCR amplification, therefore, was observed in all five unbuffered formalin-fixed, paraffin-embedded thyroid tissue samples through the preheating of RNA in citrate buffer (pH 4.0).

Discussion

Multiple papers have reported improvement in efficiency of RNA extraction from buffered formalin-fixed, paraffin-embedded tissue. Few reports, however, have

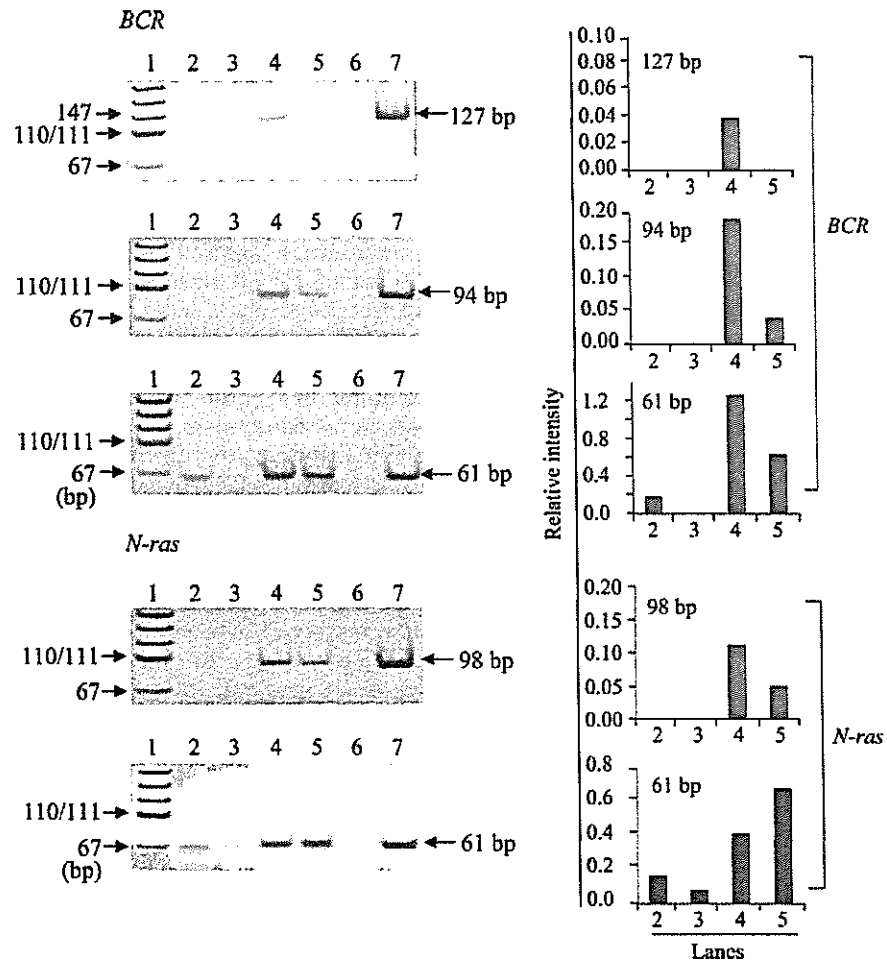

Figure 5 Effect of concentration of citrate buffer on RT-PCR amplification of RNA isolated from archival thyroid tissues. RT-PCR amplification of RNA preheated at 70C for 30 min in various concentrations of citrate buffer with pH 4.0 (Lane 3, 50 mM; Lane 4, 10 mM; Lane 5, 2 mM) was performed on three different sizes of fragments in the *BCR* gene and two different sizes of fragments in the *N-ras* gene. Lane 2, no preheating; Lane 6, negative control; Lane 7, positive control; Lane 1, pUC19-MspI digest for DNA size marker.

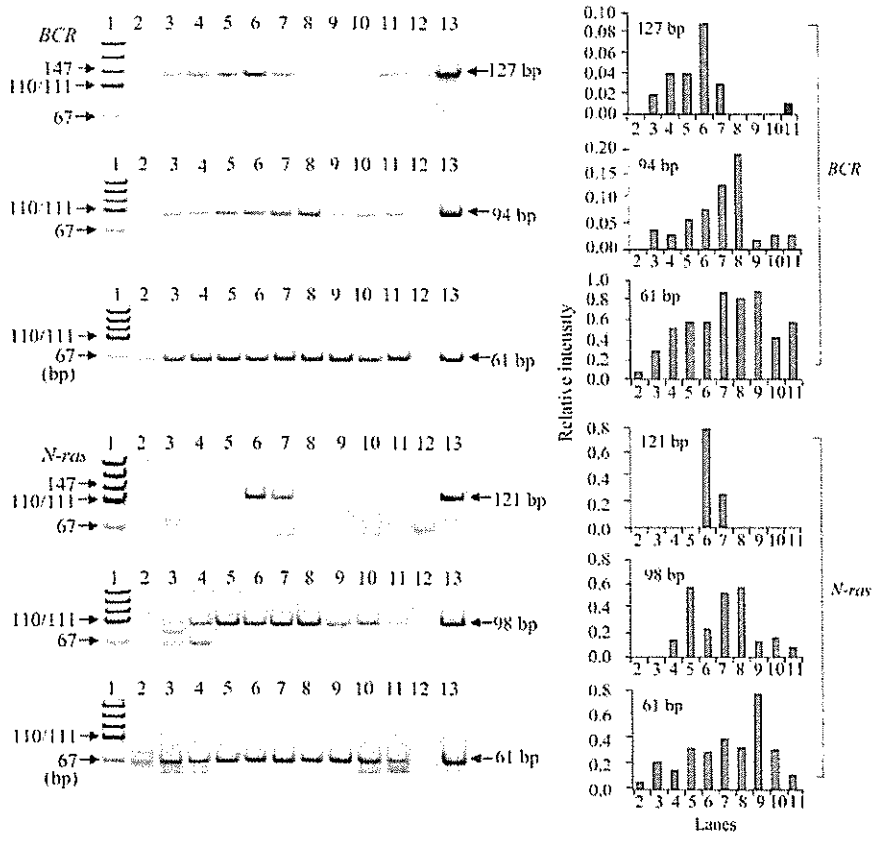

Figure 6 Effect of preheating time on RT-PCR amplification. RT-PCR amplification of RNA preheated at 70C in citrate buffer (pH 4.0) for various preheating times (Lane 2, 0 min; Lane 3, 10 min; Lane 4, 20 min; Lane 5, 30 min; Lane 6, 45 min; Lane 7, 60 min; Lane 8, 90 min; Lane 9, 120 min) was done for different lengths of fragments in *BCR* and *N-ras*. Lanes 10 and 11, preheated with TE for 30 min and 60 min; Lane 12, negative control; Lane 13, positive control; Lane 1, pUC19-MspI digest.

reported on elimination of modification induced by buffered formalin fixation, although RT-PCR amplification of RNA extracted from archival formalin-fixed, paraffin-embedded tissue was hindered not only by degradation of RNA but also by modification of RNA bases by formalin. Preheating of RNA in TE buffer (pH 7.0) restored the template activity of RNA extracted from buffered formalin-fixed tissue where clear bands of 18S and 28S rRNA were still detected with partial degradation (Masuda et al. 1999). The reaction between formaldehyde and nucleotide monomers takes place in two steps. Primary reaction is to form labile methylol-derivatives by addition of formaldehyde group to NH-group of bases. Secondary slow reaction is to give rise to stable methylene derivatives in only amino purines (Feldman 1973; Auerbach et al. 1977). The reaction between formaldehyde and RNA is also thought to occur in the same manner. In fact, matrix-assisted laser desorption/ionization–time of flight (MALDI-TOF) analysis has indicated that all four bases of RNA treated with buffered formalin were modified mainly by addition of mono-methylol groups (Masuda et al. 1999). Modification of nucleotides by addition of methylol groups is a reversible reaction: heating of RNA with 10 mM TE buffer (pH 7.0) at 70C results in removal of methylol derivatives from bases (Masuda et al. 1999).

Our results indicate that efficiency of RT-PCR amplification with degraded RNA extracted from long-term preserved unbuffered formalin-fixed, paraffin-embedded tissue specimens (for 19 to 21 years) is improved by the heating of RNA in citrate buffer prior to cDNA synthesis. This enhanced efficiency was possibly caused by RNA modification elimination and subsequent RNA template activity restoration.

Fragment sizes of ~60 bp can be amplified successfully at a rate of ~80% by RT-PCR, even when using RNA extracted from archival formalin-fixed, paraffin-embedded tissue samples stored for a long period. However, as in the case of amplification of the *N-ras* gene in two samples used in this study, archival tissue samples still remain in which a weak band is only vaguely observed or not detected even when fragment size by RT-PCR amplification is ~60 bp.

Furthermore, when amplicon size is very small, it is often difficult to design primers in restricted regions such as fusion points. Therefore, increased efficiency of RT-PCR amplification by the preheating of RNA is most effective when only limited quantities of archival formalin-fixed, paraffin-embedded tissue samples are

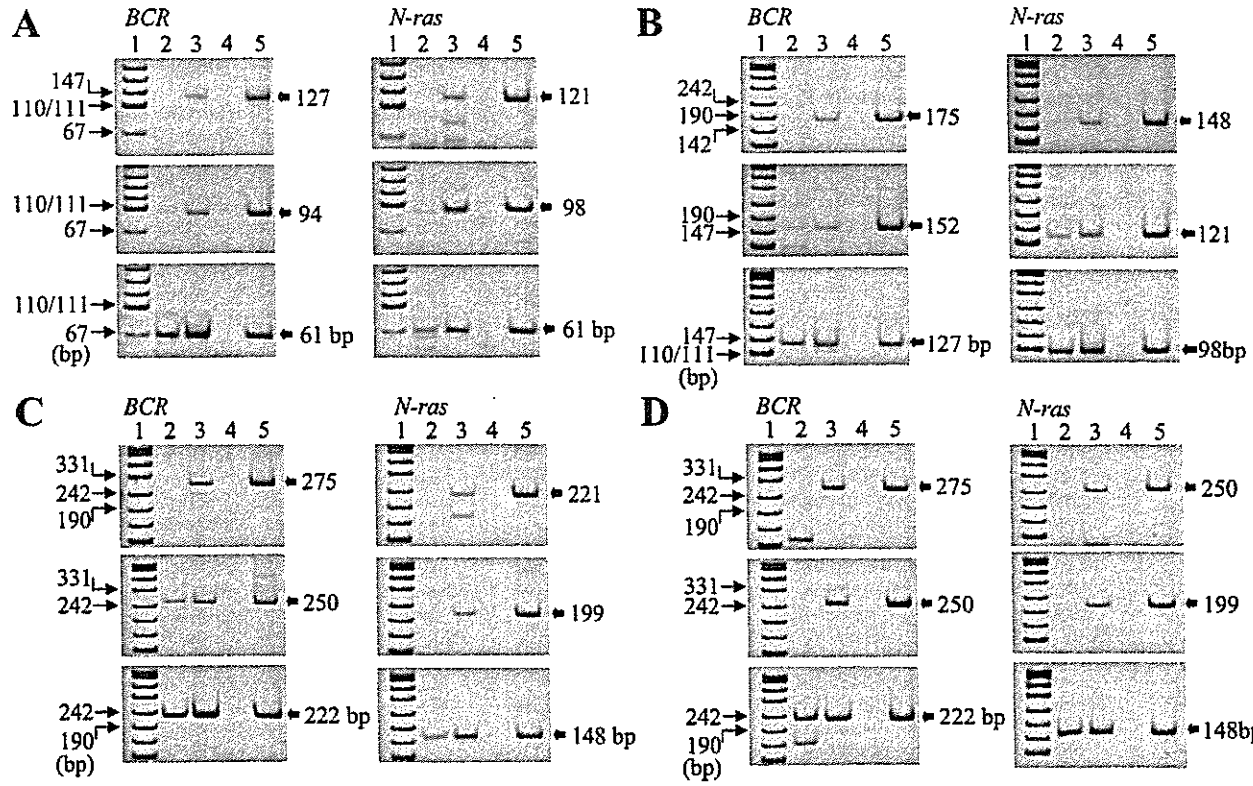

Figure 7 Application of preheating in citrate buffer (pH 4.0) to RT-PCR amplification of RNA extracted from the other four archival thyroid tissues (A–D). RNA was heated in citrate buffer at 70C for 45 min before cDNA was synthesized (Lane 3). Lane 2, no preheating; Lane 4, negative control; Lane 5, positive control; Lane 1, pUC19-MspI digest.

available for study or when the designing of primers in restricted regions cannot be avoided.

Heat treatment with alkaline solution (pH 9–12) for DNA extraction from archival formalin-fixed, paraffin-embedded tissue increased the efficiency of DNA extraction, resulting in enhanced PCR amplification (Shi et al. 2002,2004). Our results demonstrate that heat treatment in citrate buffer with pH ranging from 3 to 6.5 improves to some extent the efficiency of RT-PCR amplification of RNA extracted from archival formalin-fixed, paraffin-embedded tissue, whereas treatment of RNA with pH solution ranging from 9 to 10 reduced the efficiency of RT-PCR amplification. These findings indicate that RNA or DNA modification induced by formalin may be removed more efficiently by preheating in acidic or alkaline buffer compared with neutralized buffer. The efficiency of RT-PCR amplification enhanced by RNA preheating in citrate buffer (pH 3–6.5) may be due to the fact that RNA is relatively stable in weak acidic solution but unstable in alkaline solution.

Treatment with highly concentrated citrate buffer reduced the efficiency of RT-PCR amplification of RNA compared with non-treated RNA. In our experiment, incubation time of 30–60 min in citrate buffer with pH 4.0 was the most efficient method for RT-PCR amplification. A longer incubation time, such as 2 hr, resulted in slightly decreased efficiency of RT-PCR amplification, suggesting that degradation of RNA may occur to some extent during the long preheating in citrate buffer at 70C.

Preheating of RNA in citrate buffer resulted in improved efficiency of RT-PCR amplification in all five archival tissue specimens examined, suggesting that this method is useful for molecular analyses of long-term preserved tissue specimens. This technique will enable the qualitative analysis such as DNA rearrangement using degraded RNA extracted from archival unbuffered formalin-fixed, paraffin-embedded tissue specimens that have been stored for more than several decades. It will shed light on the retrospective studies of rare cancers or cancers associated with exposure to uncommon past events such as Thorotrast treatment, nuclear power station accidents, or atomic bombings.

Acknowledgments

The Radiation Effects Research Foundation (RERF), Hiroshima and Nagasaki, Japan is a private, non-profit foundation funded by the Japanese Ministry of Health, Labor and Welfare (MHLW) and the U.S. Department of Energy (DOE),

the latter through the National Academy of Sciences. This publication was supported by RERF Research Protocol (RP) No. 5-02 and in part by Grant-in-Aid for Japan–U.S. Cooperative Science Program Joint Project from the Japan Society for the Promotion of Science, for Scientific Research from the Ministry of Education, Culture, Sports, Science and Technology of Japan, and for Cancer Research from the Ministry of Health, Labor and Welfare of Japan.

We thank Shiho Yano and Kanya Hamasaki for excellent technical assistance.

Literature Cited

Auerbach C, Moutschen-Dahmen M, Moutschen J (1977) Genetic and cytogenetical effects of formaldehyde and related compounds. Mutat Res 39:317–362

Bresters D, Cuypers HTM, Reesink HW, Chamuleau RAFM, Schipper MEI, Boeser-Nunnink BDM, Lelie PN, et al. (1992) Detection of hepatitis C viral RNA sequences in fresh and paraffin-embedded liver biopsy specimens of non-A, non-B hepatitis patients. J Hepatol 15:391–395

Bresters D, Schipper MEI, Reesink HW, Boeser-Nunnink BDM, Cuypers HTM (1994) The duration of fixation influences the yield of HCV cDNA-PCR products from formalin-embedded liver tissue. J Virol Methods 48:267–272

Byers R, Roebuck J, Sakhinia E, Hoyland J (2004) PolyA PCR amplification of cDNA from RNA from formalin-fixed paraffin-embedded tissue. Diagn Mol Pathol 13:144–150

Cohen CD, Gröne H-J, Gröne EF, Nelson P, Schlöndorff D, Kretzler M (2002) Laser microdissection and gene expression analysis on formaldehyde-fixed archival tissue. Kidney Int 61:125–132

Cronin M, Pho M, Dutta D, Stephans JC, Shak S, Kiefer MC, Esteban JM, et al. (2004) Measurement of gene expression in archival paraffin-embedded tissues: development and performance of a 92-gene reverse transcriptase-polymerase chain reaction assay. Am J Pathol 164:35–42

Feldman MY (1973) Reactions of nucleic acids and nucleoproteins with formaldehyde. Prog Nucleic Acid Res Mol Biol 13:1–49

Finke J, Fritzen R, Ternes P, Lange W, Dölken G (1993) An improved strategy and a useful housekeeping gene for RNA analysis from formalin-fixed, paraffin-embedded tissues by PCR. Biotechniques 14:448–453

Forsthoefel KF, Papp AC, Snyder PJ, Prior TW (1992) Optimization of DNA extraction from formalin-fixed tissue and its clinical application in Duchenne muscular dystrophy. Am J Clin Pathol 98:98–104

Frank TS, Svoboda-Newman SM, His ED (1996) Comparison of methods for extracting DNA from formalin-fixed paraffin sections for nonisotopic PCR. Diagn Mol Pathol 5:220–224

Goldsworthy SM, Stockton PS, Trempus CS, Foley JF, Maronpot RR (1999) Effects of fixation on RNA extraction and amplification from laser capture microdissected tissue. Mol Carcinog 25: 86–91

Jackson DP, Lewis FA, Taylor GR, Boylston AW, Quirke P (1990) Tissue extraction of DNA and RNA and analysis by the polymerase chain reaction. J Clin Pathol 43:499–504

Kim J-O, Kim H-N, Hwang M-H, Shin H-I, Kim S-Y, Park R-W, Park E-Y, et al. (2003) Differential gene expression analysis using paraffin-embedded tissues after laser microdissection. J Cell Biochem 90:998–1006

Koopmans M, Monroe S, Coffield LM, Zaki SR (1993) Optimization of extraction and PCR amplification of RNA extracts from paraffin-embedded tissue in different fixatives. J Virol Methods 43:189–204

Körbler T, Grković M, Dominis M, Antica M (2003) A simple method for RNA isolation from formalin-fixed and paraffin-embedded lymphatic tissues. Exp Mol Pathol 74:336–340

Lehmann U, Kreipe H (2001) Real-time PCR analysis of DNA and RNA extracted from formalin-fixed and paraffin-embedded biopsies. Methods 25:409–418

Masuda N, Ohnishi T, Kawamoto S, Monden M, Okubo K (1999) Analysis of chemical modification of RNA from formalin-fixed samples and optimization of molecular biology applications for such samples. Nucleic Acids Res 27:4436–4443

Mies C (1994) Molecular biological analysis of paraffin-embedded tissues. Hum Pathol 25:550–560

Park YN, Abe K, Li H, Hsuih T, Thung SN, Zhang DY (1996) Detection of hepatitis C virus RNA using ligation-dependent polymerase chain reaction in formalin-fixed, paraffin-embedded liver tissues. Am J Pathol 149:1485–1491

Rupp GM, Locker J (1988) Purification and analysis of RNA from paraffin-embedded tissues. Biotechniques 6:56–60

Shi S-R, Cote RJ, Wu L, Liu C, Datar R, Shi Y, Liu D, et al. (2002) DNA extraction from archival formalin-fixed, paraffin-embedded tissue sections based on the antigen retrieval principle: heating under the influence of pH. J Histochem Cytochem 50: 1005–1011

Shi S-R, Datar R, Liu C, Wu L, Zhang Z, Cote RJ, Talor CR (2004) DNA extraction from archival formalin-fixed, paraffin-embedded tissues: heat-induced retrieval in alkaline solution. Histochem Cell Biol 122:211–218

Specht K, Richter T, Müller U, Walch A, Werner M, Hofler H (2001) Quantitative gene expression analysis in microdissected archival formalin-fixed and paraffin-embedded tumor tissue. Am J Pathol 158:419–429

Weizäcker FV, Labeit S, Koch HK, Oehlert W, Gerok W, Blum HE (1991) A simple and rapid method for the detection of RNA in formalin-fixed, paraffin-embedded tissues by PCR amplification. Biochem Biophys Commun 174:176–180

The Journal of Histochemistry & Cytochemistry

Short-Term Culture and γH2AX Flow Cytometry Determine Differences in Individual Radiosensitivity in Human Peripheral T Lymphocytes

Kanya Hamasaki,[1] Kazue Imai,[1] Kei Nakachi,[1] Norio Takahashi,[2] Yoshiaki Kodama,[2] and Yoichiro Kusunoki[1]*

[1]*Department of Radiobiology/Molecular Epidemiology, Radiation Effects Research Foundation, Hiroshima, Japan*

[2]*Department of Genetics, Radiation Effects Research Foundation, Hiroshima, Japan*

Histone H2AX, a subfamily of histone H2A, is phosphorylated and forms proteinaceous repair foci at the sites of DNA double-strand breaks in response to genotoxic insults, such as ionizing radiation. This process is believed to play a key role in the repair of DNA damage. In this study, we established a flow cytometry (FCM) system for measuring radiation-induced phosphorylated histone H2AX (γH2AX) in cultured human T lymphocytes to evaluate individual radiation sensitivity in vitro. Irradiation of short-term (~7 days) cultured T lymphocytes exhibited significant interindividual, but not interexperimental, differences in the cellular content of γH2AX 6 hr after 4 Gy of X-irradiation in three independent experiments using peripheral blood lymphocytes from six healthy donors. However, these differences were not as marked in uncultured lymphocytes, or lymphocytes that were cultured for a prolonged period (~13 days). The variation of γH2AX focus formation in lymphocytes of individuals was reproducible, with differences reaching about 1.5-fold following 7 days of culture. Therefore, the FCM-based γH2AX measurement appeared to reflect both the temporal course and the amount of DNA damage within the irradiated lymphocytes. Further, we confirmed that the differences in residual lymphocyte subsets were not involved in individual radiosensitivity. These results suggest that the FCM-based γH2AX assay using cultured T lymphocytes might be useful for the rapid and reliable assessment of individual radiation sensitivity involved in DNA damage repair. Environ. Mol. Mutagen. 48:38–47, 2007.

Key words: DNA repair; peripheral blood; radiation effect

INTRODUCTION

It is believed that interindividual variability in the cellular responses to genotoxic agents, e.g., ionizing radiation, is a critical element in reliably estimating cancer risks in exposed individuals and populations. To assess individual sensitivity to radiation exposure in vitro, different endpoints measuring radiation-induced cellular damage, such as DNA strand-breaks, chromosomal damage, and lethality, have been studied. For example, increased radiation sensitivity to chromosome damage has been observed not only in a number of heritable cancer-prone disorders, but also in a significant proportion of sporadic cancer cases [Parshad et al., 1996; Scott et al., 1998, 1999; Roberts et al., 1999; Terzoudi et al., 2000]. A positive association has been demonstrated for humans between chromosome aberration frequency in peripheral blood T lymphocytes and cancer susceptibility [Hagmar et al., 2004]. Further, a possible positive correlation has been recognized between the radiosensitivity of lymphocytes irradiated in vitro and in vivo exposure, specifically when survival is used as the endpoint [West et al., 2001]. Analyses of chromosomal aberrations and estimates of survival responses, which these studies used, are sensitive and reliable biomarkers for the assessment of cellular damage, but they require considerable labor and a high degree of technical skill. Bioindicators of an individual's inherent

Grant sponsors: Ministry of Education, Culture, Sports, Science, and Technology of Japan; The Ministry of Health, Labour and Welfare.

*Correspondence to: Yoichiro Kusunoki, PhD, Department of Radiobiology/Molecular Epidemiology, Radiation Effects Research Foundation, 5-2 Hijiyama Park, Minami-ku, Hiroshima 732-0815, Japan.
E-mail: ykusunok@rerf.or.jp

Received 24 August 2006; provisionaly accepted 22 September 2006; and in final form 6 October 2006

DOI 10.1002/em.20273

Published online 12 December 2006 in Wiley InterScience (www.interscience.wiley.com).

radiosensitivity, and perhaps cancer risk that is easily and reliably measured, need to be identified and developed, preferably using high throughput assay platforms and highly objective criteria to quantitate endpoints.

It is well known that DNA double-strand breaks (DSBs) in cell nuclei are generated by sufficiently intense exposure to genotoxic agents, including ionizing radiation. In response to DSB generation, histone H2AX, a subfamily of histone H2A, is rapidly phosphorylated by members of the PI3 kinase family (ATM, DNA-PK, and ATR) and forms proteinaceous foci that cover large regions (at least 2 Mb) surrounding DSB sites [Rogakou et al., 1998]. Antibody-specific immunofluorescence has been used to visualize the time course of phosphorylated H2AX (γH2AX) development and regression in irradiated cell nuclei and indicates that foci continue to grow for about 1 hr after irradiation and then decrease in both size and number as DSB-rejoining proceeds in damaged cells. This process is believed to be critical to cellular repair of DNA damage [Paull et al., 2000; Celeste et al., 2002, 2003; Kobayashi, 2004]. Since the number of γH2AX foci closely corresponds to the number of DSBs in cells [Rogakou et al., 1999], counting γH2AX foci has frequently been used to estimate DSBs in cells following genotoxic stress and the subsequent repair of DNA damage. The γH2AX focus-based assay is generally regarded as being more sensitive in detecting DSBs than more conventional assays, such as pulse-field gel electrophoresis (PFGE), neutral single cell electrophoresis (Comet assay), or the DNA elution assay [Takahashi and Ohnishi, 2005].

Flow cytometry (FCM)-based γH2AX assays, which have high-speed and high-sensitivity, have been developed previously, but applied solely to assessing the generation and repair of DSBs in various tumor cell lines [MacPhail et al., 2003a,b; Banath et al., 2004]. In this study, we attempted to establish a reliable and straightforward system for detecting in vitro radiation-induced DSBs in cultured T lymphocytes from normal healthy humans using γH2AX FCM. Further, we attempted to validate the assay's applicability for analyzing individual radiation sensitivity in human populations.

MATERIALS AND METHODS

Cell Culture

Venous peripheral blood was obtained with informed consent from six healthy adults (four males aged 33, 38, 49, and 49, and two females aged 40 and 49) at our laboratory. We obtained approval from the Human Investigation Committee of the Radiation Effects Research Foundation at the time this study was carried out. Peripheral blood mononuclear cells (PBMCs) were separated by Ficoll-Hypaque density gradient centrifugation (LSM Lymphocyte Separation Medium; MP Biomedicals, Aurora, OH). T-lymphocyte cultures were established and maintained as described previously [Kushiro et al., 1992]. In brief, separated PBMCs were distributed into each well of a 24-well plate (Corning, Corning, NY) at 5×10^5 cells/well with 2 ml GIT medium (Wako Pure Chemical Industry, Osaka, Japan) containing 10% fetal bovine serum (FBS; Intergen, New York, NY), 2% L-glutamine (Invitrogen, Carlbad, CA), 2% penicillin–streptomycin (Invitrogen), 1:3,200 Phytohemagglutinin (PHA; Difco Laboratories, Detroit, MI), and 10 ng/ml human recombinant interleukin-2 (rIL-2; Pepro Tech, London, UK), and cultured for 7 days at 37°C in 5% CO_2 and 95% air. After 7 days of culture, propagated T lymphocytes were collected and resuspended in fresh media for analyses. B-lymphoblastoid cell lines were established by incubating PBMCs with a culture supernatant of Epstein–Barr virus-producing B95-8 cell lines [Kusunoki et al., 1995]. The B-cell lines were maintained by weekly replacement of part of the culture with fresh GIT medium, supplemented with 10% FBS, 2% L-glutamine, and antibiotics.

X-Irradiation

Cells were resuspended in wells of 24-well plates at an approximate cell concentration of 1×10^6 ml, irradiated with 1, 2, 4, or 8 Gy of X-rays, and further cultured for 1, 2, 6, or 24 hr after X-irradiation. Irradiation was performed at a dose rate of 0.7 Gy/min at room temperature using an X-ray irradiator (HF-320; Shimazu, Kyoto, Japan) equipped with 0.5-mm Al and 0.3-mm Cu filters at 220 kVp and 8 mA. To ensure accurate comparison among different samples, the samples were irradiated simultaneously.

γH2AX FCM

Cells cultured after X-irradiation were fixed in 70% ethanol at a cell concentration of 4×10^6 ml and kept at −20°C until use. Fixed cells (50 μl, 2×10^5) were added with 150 μl phosphate buffered saline (PBS; Sigma-Aldrich, St. Louis, MO) in the wells of a 96-well U-bottom plate (Becton Dickinson, Franklin Lakes, NJ) and centrifuged at 450*g* for 5 min. The cells were washed twice with PBS and then resuspended in 50 μl permeabilization buffer (0.5% saponin, 10 mM HEPES, pH 7.4, 140 mM NaCl, 2.5 mM $CaCl_2$). Following incubation with 4 μl mouse monoclonal antiphosphohistone H2A.X (Ser139) antibody (Upstate, Lake Placid, NY) diluted 1:100 with PBS containing 1% FBS, and 0.01% NaN_3 for 20 min at room temperature, the cells were washed with PBS containing 0.1% saponin. Subsequently, 40 μl secondary antibody, Alexa 488 $F(ab')_2$ fragment of goat antimouse IgG (H + L) (Molecular Probes, Eugene, OR) diluted 1:50 with PBS (containing 1% FBS, 0.01% NaN_3), was added to the cell pellet, and the cell suspension was incubated for 20 min at room temperature. After the reaction, the cells were washed and resuspended in PBS containing 1% FCS, 0.01% NaN_3 containing 5 μg/ml propidium iodide (PI; Wako Pure Chemical Industry), and 40 ng/ml RNase A (MP Biomedicals, Aurora, OH) for at least 30 min prior to FCM. Expression levels of γH2AX in 1×10^4 cells were analyzed using a FACScan (BD Biosciences, Franklin Lakes, NJ). Since it was necessary to compare γH2AX levels within lymphocytes of six healthy adults under the same experimental conditions, all samples were measured on the same day. Data analysis was conducted using Flowjo software (Tree Star, Ashland, OR). Radiation-induced γH2AX levels were determined by relative γH2AX fluorescence intensities, i.e., differences between the mean fluorescence of unirradiated and irradiated cells. In a selected number of experiments, appropriate fractions of cultured T lymphocytes were sorted with the cell sorter, JSAN (Bay Bioscience, Kobe, Japan), and subsequently analyzed microscopically. For these cell sorting experiments we used 4′ 6-diamidino-2-phenylindole dihydrochloride hydrate (DAPI; Wako Pure Chemical Industries) at 1 μg/ml instead of PI for DNA staining.

Lymphocyte Viability and Phenotype

Cultured T cells were stained with FITC-labeled anti-Annexin V (MBL, Nagoya, Japan) and PI, and subsequently assessed for viability using a FCM method described previously [Ohara et al., 2004]. Lymphocyte subsets in both uncultured and cultured cell populations were examined using

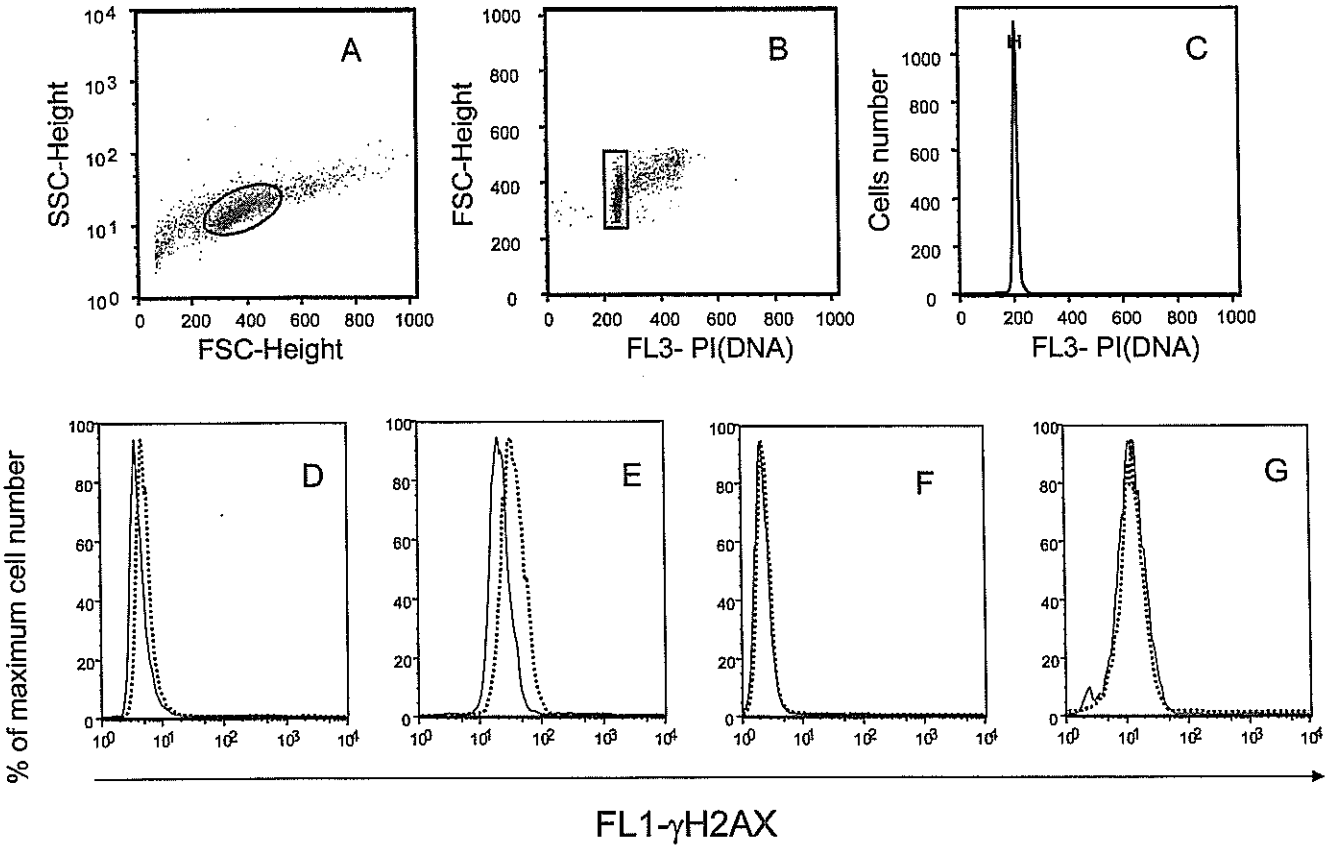

Fig. 1. Flow cytometry (FCM) analysis of phosphorylated H2AX (γH2AX) in cultured T lymphocytes and uncultured lymphocytes 6 hr after 0 or 4 Gy of X-irradiation. Dashed (Donor 2) and solid (Donor 6) lines indicate γH2AX histograms in two individuals who showed the second highest and the lowest sensitivity to radiation-induced γH2AX expression among six healthy adults (Fig. 5). (A) Gating on the viable single-cell events based on forward and side light scattering (FSC and SSC). (B) Subsequent rough gating on the diploid cell fraction. (C) Final strict gating on G1 cells showing the FL3 (PI) peak channel ±20 fluorescence units. (D) γH2AX histograms in the strictly gated G1-cell population of unirradiated cultured T lymphocytes. (E) γH2AX histograms in 4 Gy irradiated cultured T lymphocytes. (F) γH2AX histograms in unirradiated fresh lymphocytes. (G) γH2AX histograms in irradiated fresh lymphocytes.

an FCM method, as described previously [Kusunoki et al., 1998]. For these analyses, cells were stained with CD3-PerCP, CD4-FITC, CD8-PECy5, CD20-PE (BD Biosciences Pharmingen, San Jose, CA), CD16-FITC, or CD45RA-PE antibodies (Beckman Coulter, Miami, FL).

T-Lymphocyte Sorting

Freshly isolated lymphocytes were stained with PE-labeled CD3, PECy7-labeled CD4, and FITC-labeled antibodies (BD Biosciences). CD3+/CD4+ and CD3+/CD8+ fractions were isolated using JSAN. The cell fractions were then cultured by the method described above, and subsequently used for γH2AX FCM analyses. The percentages of viable CD3+/CD4+ and CD3+/CD8+ cell fractions recovered after 7 days of culture were 98% and 99%, respectively.

Fluorescence Microscopy Analysis

Cells stained with anti-γH2AX and Alexa 488-labeled secondary antibodies, as described above, were cytocentrifuged onto glass slides (Cytospin 3; Shandon, Cheshire, UK), air-dried and mounted with an antifade solution containing 125 ng/ml DAPI.

The cells were visualized with a fluorescence microscope, and representative images were captured and automatically analyzed using Image Pro Plus 4.5 software (Planetron, Tokyo, Japan). The software incorporated a macroprogram designed to aid in enumerating the number of γH2AX foci per cell by identifying nucleus position and the associated number of foci via thresholding the area and diameter of foci.

Statistical Analysis

Distributions of values for γH2AX levels were analyzed for interindividual or interexperimental variations by one-way analyses of variance (ANOVA). Associations between levels of γH2AX measured by FCM and the number of γH2AX foci per cell measured microscopically in appropriate cell fractions were analyzed using the Jonckheere-Terpstra test (SPSS ver. 13.0; SPSS, Chicago, IL).

RESULTS

γH2AX FCM Gated on G0/G1 Phase Cells

It is known that γH2AX focus formation appears not only in cells in which DNA DSBs have been induced, but also in those undergoing DNA synthesis and mitosis [Ichijima et al., 2005; McManus and Hendzel, 2005] or apoptosis [MacPhail et al., 2003b; Mukherjee et al., 2006].

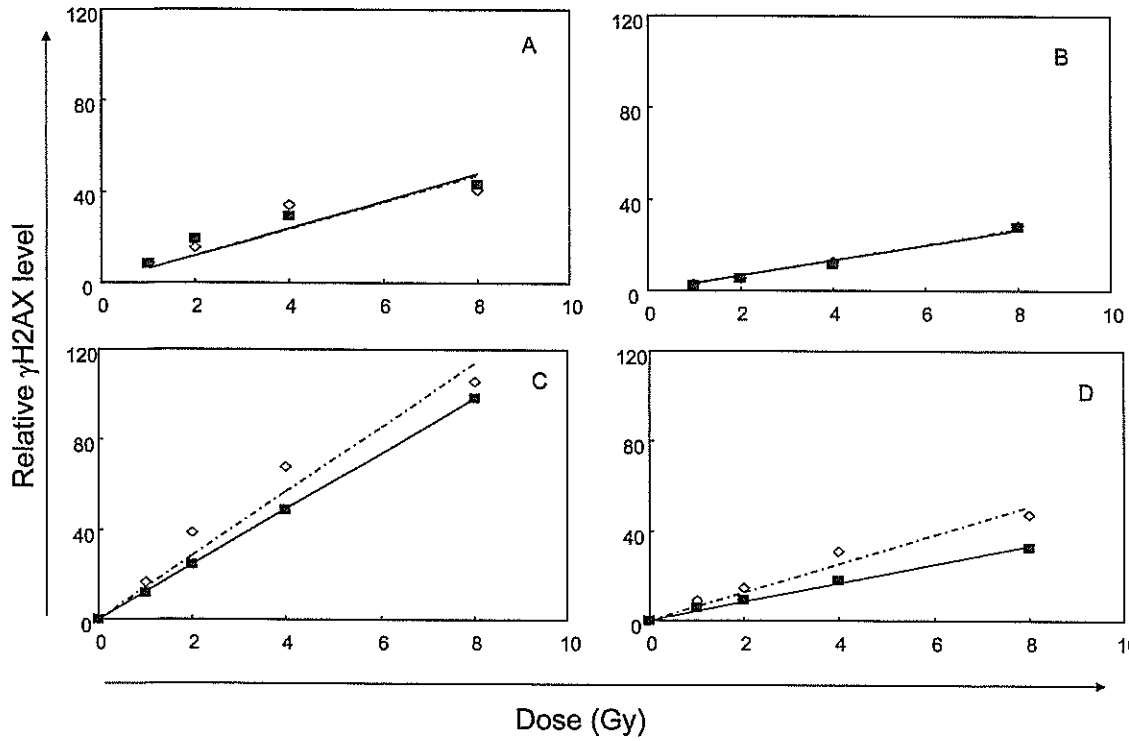

Fig. 2. Dose responses of γH2AX levels in uncultured lymphocytes (A,B) and cultured T lymphocytes (C,D) from Donor 2 (dashed-dotted lines) and Donor 6 (solid lines). Cultured T lymphocytes were irradiated with 0, 1, 2, 4, and 8 Gy of X-rays and analyzed for γH2AX expression 1 hr (A,C) and 6 hr (B,D) after irradiation. There was a significant linear correlation ($r > 0.86$) between relative γH2AX level and radiation dose for each donor both 1 and 6 hr after irradiation.

To ensure the accuracy of measurements specific for radiation-induced γH2AX, X-irradiated cells were simultaneously analyzed for γH2AX expression and DNA content by FCM. The γH2AX levels were determined in cell fractions gated on the G0/G1 phase. Figure 1 shows an example of FCM used for determining the γH2AX level in irradiated cells. After gating on viable single-cell events based on forward and side light scattering (Fig. 1A) and subsequent gating on diploid cells (Fig. 1B), G0/G1 phase cells were clearly distinguished by their DNA content, as reflected by peak channel fluorescence (±20 fluorescence units) from the other events (Fig. 1C). The γH2AX level in the G0/G1 phase cell populations was determined by the geometric mean of γH2AX fluorescence.

Sensitivity of γH2AX FCM Using Cultured and Uncultured Lymphocyte Populations

Measurements of radiation-induced γH2AX levels within cultured T lymphocytes and uncultured fresh lymphocytes were carried out and validated using FCM. Figure 1 shows typical FCM patterns observed in cultured and uncultured cells 6 hr after either 0 or 4 Gy of X-irradiation. Donors 2 and 6 provided the cells for these experiments, and as described later, they showed the second highest and the lowest sensitivities to radiation-induced γH2AX expression among the six individuals we studied. We detected significant differences in the levels of γH2AX fluorescence levels between these two individuals in T-lymphocytes cultured for 7 days prior to irradiation, whereas there was no obvious difference in γH2AX expression level when we used uncultured lymphocytes (Fig. 2). A linear relationship existed between radiation dose and γH2AX expression level in both cultured and uncultured lymphocytes from both of these individuals (Fig. 2). One hour after irradiation, the radiation dose effect in uncultured lymphocytes was about half of that found in cultured T lymphocytes (Fig. 2A). Six hours after irradiation, a similar difference also was observed between uncultured and cultured lymphocytes for Donor 2, whereas the dose effect difference was smaller for Donor 6 (Fig. 2C). We also observed by FCM a clear difference in the dose response of γH2AX expression by cultured T lymphocytes of these two individuals when assayed at 1 and 6 hr after irradiation. By contrast, the difference in the dose response was not obvious in uncultured lymphocytes from the same donors.

Although we also tested EBV-transformed B-cell lines for γH2AX expression after irradiation, and obtained similar dose responses to those of cultured T lymphocytes, the responses of several B-cell lines prepared from the same six blood donors were not as consistent in terms of the γH2AX levels produced by given doses of irradiation (data not shown). These results suggest that in terms of

analyzing individual variability in the level of radiation-induced γH2AX expression by FCM, cultured T lymphocytes are preferable to the other sources, in terms of sensitivity and reliability.

Preirradiation Cultures and Postirradiation Time Course

Changes of γH2AX levels in cultured T lymphocytes from the six healthy adults were analyzed at 1, 2, 6, and 24 hr after 4 Gy irradiation in three independent experiments. Results from a typical experiment are shown in Figure 3. The γH2AX level reached a peak 1 or 2 hr after radiation exposure and then gradually decreased with time. Even though the time-course pattern did not differ appreciably among the individuals, variations in γH2AX levels were observed at various times following irradiation. For example, γH2AX levels, 6 hr after 4 Gy irradiation, differed by about 1.5-fold in the highest vs. the lowest responding donors. Next, we examined whether the period of T-cell culture before irradiation affected the reliability of γH2AX measurement for individual variability. For this experiment, cells from the two individuals who showed the second highest and the lowest γH2AX levels at 6 hr after irradiation were used (i.e., as does the experiment shown in Figure 3; Donors 2 and 6). As shown in Figure 4, similar differences between these two individuals were detected when T lymphocytes were cultured for 5–13 days before irradiation. However, the difference was not as obvious in T lymphocytes cultured for 13 days as in those cultured for 5–10 days (Fig. 4).

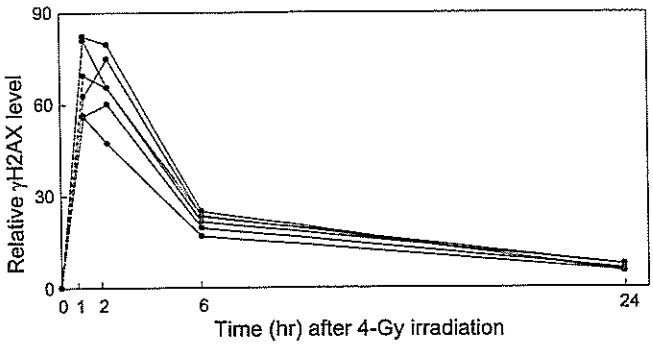

Fig. 3. Time course of radiation-induced γH2AX expression in cultured T lymphocytes from six healthy individuals. Cellular γH2AX levels were measured 1, 2, 6, and 24 hr after 4 Gy irradiation. The vertical axis indicates relative γH2AX fluorescence intensity, which is the geometrical mean of the γH2AX level in irradiated cells minus that in unirradiated cells.

Interindividual and Interexperimental Variations in γH2AX Level

To assess whether individual differences in radiation-induced γH2AX levels could be observed reproducibly, three independent experiments were carried out using T lymphocytes obtained at different times from the same six individuals. Lymphocytes were cultured for 7 days before 4 Gy irradiation, and both interindividual and interexperimental variations were analyzed statistically for each time point after irradiation. Interindividual variation in radiation-induced γH2AX levels was highly significant for every time point (Fig. 5). Although interexperimental varia-

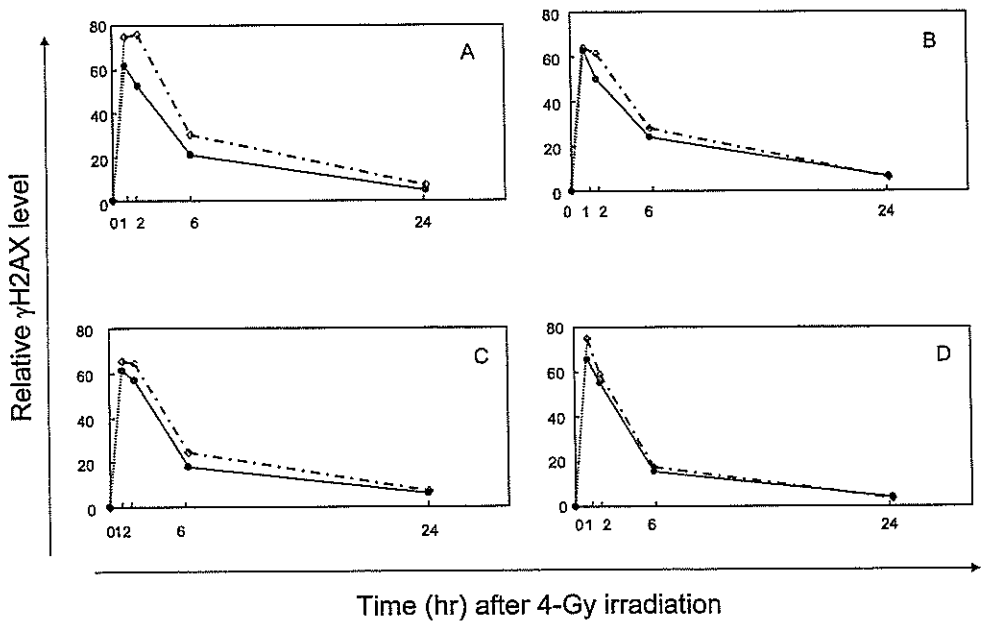

Fig. 4. Time course of levels of radiation-induced γH2AX expression in T lymphocytes cultured for 5 (A), 7 (B), 10 (C), and 13 (D) days from Donors 2 (dashed-dotted lines) and 6 (solid lines). γH2AX levels were measured 1, 2, 6, and 24 hr after 4 Gy irradiation. The vertical axis indicates relative γH2AX intensity, which is the geometrical mean of the γH2AX level in irradiated cells minus that in unirradiated cells.

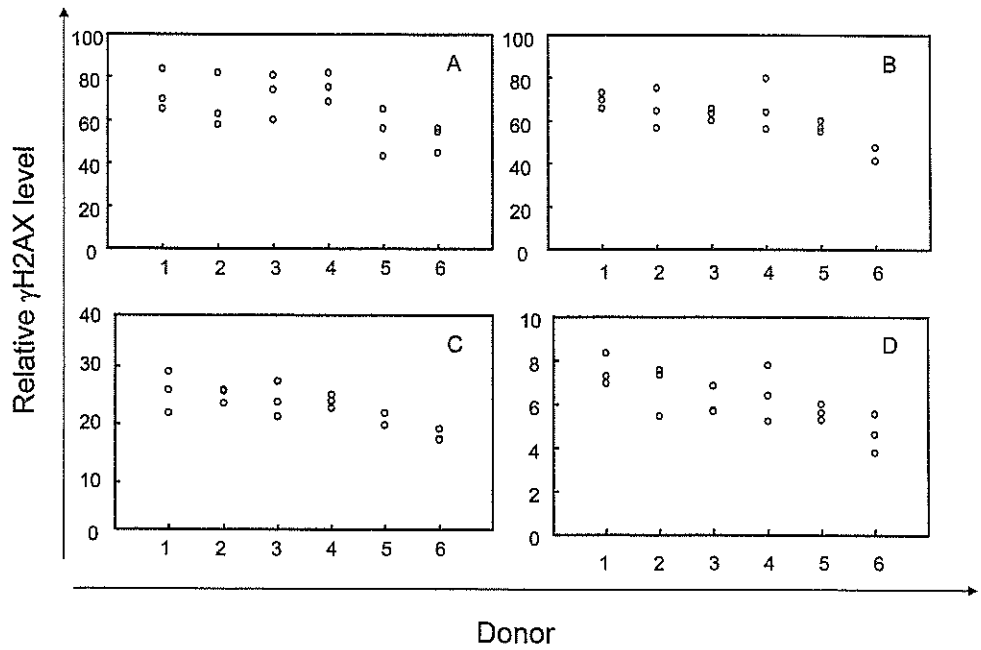

Fig. 5. Variability in the level of radiation-induced γH2AX among six healthy adults. Three independent experiments were carried out using T lymphocytes obtained from the same six individuals and cultured for 7 days before 4 Gy irradiation. Values obtained from the same experiment are plotted with the same symbols. Distributions of individual values for radiation-induced γH2AX level were analyzed for interindividual and interexperimental variation by one-way analysis of variance (ANOVA). (A) Relative γH2AX levels 1 hr after irradiation. Interindividual variability: $F = 8.46$; $P = 0.002$. Interexperimental variability: $F = 11.5$; $P = 0.003$. (B) The levels, 2 hr after irradiation. Interindividual variability: $F = 7.99$; $P = 0.003$. Interexperimental variability: $F = 3.13$; $P = 0.088$. (C) The levels 6 hr after irradiation. Interindividual variability: $F = 6.23$; $P = 0.007$. Interexperimental variability: $F = 1.64$; $P = 0.243$. (D) The levels 24 hr after irradiation. Interindividual variability: $F = 5.25$; $P = 0.013$. Interexperimental variability: $F = 3.64$; $P = 0.065$.

tion was significant, or marginally so, for 1 and 2 hr after irradiation, there was no significant interexperimental variation in the γH2AX level 6 hr after irradiation. These results suggest that for the assessment of individual radiation sensitivity relative to radiation-induced γH2AX levels, measurements tested at 6 hr after irradiation are the most reliable.

Relationship Between γH2AX Level Measured by FCM and Number of γH2AX Foci Visualized by Microscopy

To ensure that the γH2AX level determined by FCM corresponded to the number of γH2AX foci in each cell, we sorted and collected three appropriate fractions showing different levels of γH2AX and counted by fluorescence microscopy the number of γH2AX foci per cell in each of the fractions collected. As shown in Figure 6, the level of γH2AX measured by FCM almost paralleled the mean number of γH2AX foci per cell in each fraction. Statistical analysis using the Jonckheere-Terpstra test indicated that there was a significant association between the values determined by these different assays ($P < 0.001$).

We also analyzed the number of γH2AX foci in irradiated cells of individuals with high and low T-cell radiosensitivity (Donors 2 and 6) and found that the γH2AX levels analyzed by FCM closely corresponded with the number of γH2AX foci observed microscopically (Fig. 7). Because the number of γH2AX foci represents the number of DSBs in irradiated cells [Rogakou et al., 1999] and positively correlates with radiosensitivity of the cells [MacPhail et al., 2003a], differences in the level of γH2AX expression 6 hr after irradiation may reflect the difference in unrepaired DSBs. It should be noted, however, that there was no indication of radiation-induced apoptosis in cultured T lymphocytes within this 6 hr postirradiation time-frame (data not shown). This suggests that the radiation-induced γH2AX expression detected in the present study by either FCM or by microscopy probably does not involve apoptosis-related events resulting from radiation exposure.

Lymphocyte Subsets and Radiation-Induced γH2AX Levels

To characterize more fully the lymphocyte pools used in the FCM-γH2AX assays, we determined the percentages of lymphocyte subsets (CD3, CD4, CD8, CD16, and CD20) before and 7 days after culture for the six individuals we studied. The cell population just before irradiation was mainly composed of CD4 (10–40%) and CD8 (60–80%) T-cell populations, and a majority of these T-cell populations expressed a low level of CD45RA, a memory-phenotype indication. Other lymphocyte populations,

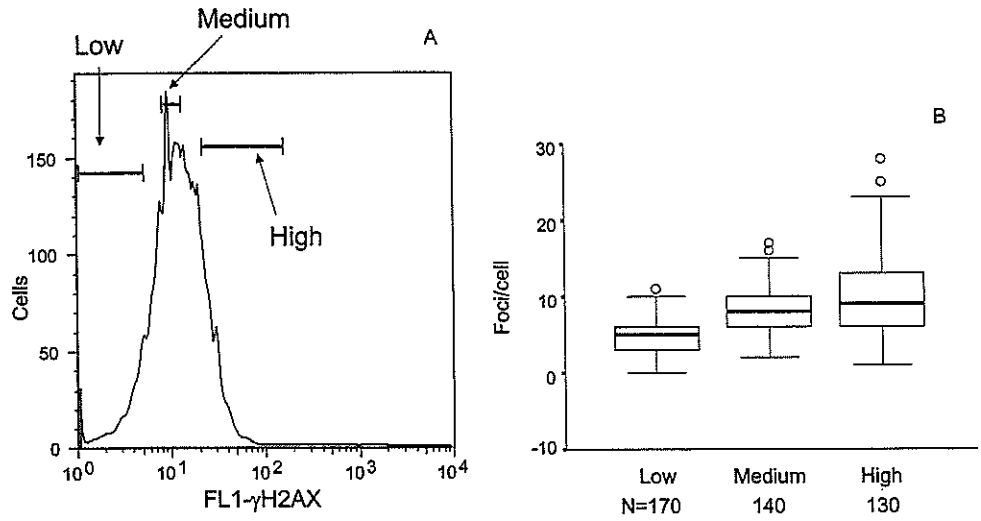

Fig. 6. Associations between γH2AX levels measured with FCM and the number of γH2AX foci determined by fluorescence microscopy in irradiated cultured T-lymphocyte fractions from one individual (Donor 2). (A) Each cell fraction showing low (1–5 fluorescence channels), medium (8–13 fluorescence channels), or high (21–160 fluorescence channels) γH2AX fluorescence intensities was sorted from cultured T lymphocytes obtained from one individual and stained for γH2AX expression 6 hr after 2 Gy irradiation. (B) Box plots of the number of foci per cell in each cell fraction. Totally 130–170 cells for each fraction were analyzed by fluorescence microscopy using Image Pro Plus 4.5 software. The horizontal line in each of the middle of boxes marks the median value in each fraction. The lower and upper edges of each box mark the 25th and 75th percentiles, respectively, and thus the central 50% of the data values fall within the range of the box. The vertical lines extending up and down from each box show the largest and the smallest values observed, respectively, and open circles mark the "outside values," which are between 1.5- and 3.0-times higher than the 75th percentile values. The Jonckheere-Terpstra test indicated that there was a significant association between γH2AX levels measured with FCM and the number of γH2AX foci determined by fluorescence microscopy ($P < 0.001$).

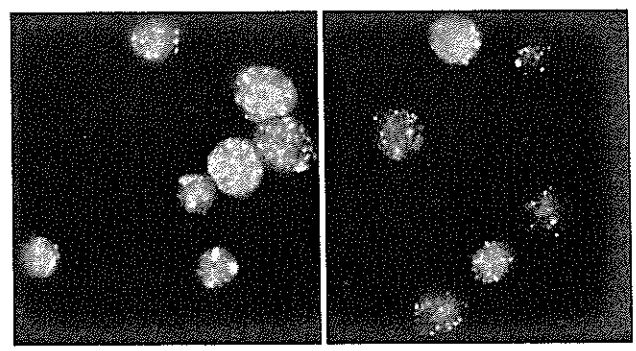

	Donor 2	Donor 6
Number of foci	1085	1082
Cells analyzed	117	147
Average (foci / cell) ± SD	9.3 ± 5.6	7.4 ± 4.9
	$p < 0.004$	

Fig. 7. Fluorescence microscopy analysis of γH2AX foci in cultured T lymphocytes from two individuals (Donors 2 and 6). The number of foci in cells was analyzed 6 hr after 4 Gy irradiation using Image Pro Plus 4.5 software. The average number of γH2AX foci per cell differed significantly between these two individuals ($P = 0.004$, the Students' t-test).

namely B and NK cells, were quite small (less than 3%). There was no obvious relationship between levels of radiation-induced γH2AX in individuals and percentages of lymphocyte subsets either before or after cell culture (data not shown). To further support the idea that differences in the CD4 and CD8 T-cell ratio does not contribute to individual differences in radiation-induced γH2AX expression, we analyzed γH2AX levels in separately cultured and irradiated CD4 and CD8 T-cell fractions from Donors 2 and 6. There was no obvious difference in the levels of radiation-induced γH2AX between CD4 and CD8 T-cell subsets in the same individuals. Difference between these individuals in terms of these subsets were apparent, i.e., γH2AX levels in CD4 and CD8 T-cell sub-

sets of Donor 2, 6 hr after 4 Gy irradiation were 32.0 and 28.7, respectively, whereas those in the comparable subsets of Donor 6 were 26.4 and 24.3, respectively. These results suggest that the differences in radiation-induced γH2AX levels in cultured T lymphocytes between individuals are not related to differences in the proportion of lymphocyte subsets within the test samples.

DISCUSSION

In this study, we established an FCM system for measuring levels of radiation-induced γH2AX in human lymphocytes to assess individual differences in radiation sensitivity to DNA damage in vitro. Currently, γH2AX focus formation is being used as a DNA damage marker, specifically for DSBs induced by exposure to various genotoxic agents, such as ionizing radiation [Rogakou et al., 1999]. γH2AX recruits other enzymes related to the DNA repair process (such as 53BP1, BRCA1, the NBS/MRE11/RAD50 complex), and thereby plays a key role in early phases of the repair of damaged cells [Paull et al., 2000; Celeste et al., 2002, 2003; Kobayashi, 2004]. We thought that by measuring cellular levels of γH2AX by high-throughput FCM, a rapid and accurate assessment of radiation sensitivity in human individuals might be possible. It has been reported that the background γH2AX level in normal cells differs at each phase of the cell cycle and appears particularly high at the S to G2/M phases [Ichijima et al., 2005; McManus and Hendzel, 2005]. Our FCM system can analyze radiation-induced γH2AX levels in cells at each phase of the cell cycle, which has been very difficult using conventional fluorescence microscopy analysis. Therefore, one major advantage of our method is that G1-phase cells, with low background γH2AX levels, can be selectively targeted for analyses.

We expect that the γH2AX FCM system established in this study will allow straightforward assessments of both individual sensitivity to radiation-induced DNA damage and individual ability to repair such DNA damage. By applying γH2AX FCM to an epidemiological follow-up study cohort, such as the A-bomb survivor populations in Hiroshima and Nagasaki, we will be able to address the important question of whether or not individuals who have lower DNA repair ability have higher mutability in response to radiation, and in turn, higher risks of radiation-related cancers.

In this study, radiation-induced γH2AX levels in blood lymphocytes appeared to be about 1.5-fold higher if the cells were cultured for 7 days prior to radiation exposure (Fig. 2). It is highly likely that growth-stimulated T lymphocytes (via PHA and IL-2) were more severely damaged by ionizing radiation than were resting peripheral blood lymphocytes. This is consistent with an earlier finding of 20-fold increases in DNA repair synthesis following ionizing irradiation of stimulated lymphocytes compared with resting lymphocytes [Lavin and Kidson, 1977]. However, it is unclear why individual differences in radiation-induced γH2AX levels can be detected more readily in cultured T lymphocytes than in freshly isolated and resting lymphocytes. This partly may be due to the relatively low γH2AX levels within resting irradiated lymphocytes that have not been growth-activated in vitro and the substantial differences in metabolic status between cultured and uncultured lymphocytes, such as specific variations in activities of DNA repair enzymes. However, it has been previously reported that the transcriptional levels of most DNA repair genes were not significantly increased in PHA-stimulated lymphocytes when compared with levels in resting lymphocytes [Mayer et al., 2002]. Therefore, it is unlikely that differences in the activity of DNA repair genes are the cause of individual differences in residual γH2AX levels in irradiated cultured T lymphocytes. Alternatively, differences in radiation sensitivity between cultured and uncultured T lymphocytes might result from differences in the ability of irradiated cells to scavenge DNA-damaging radicals induced by ionizing radiation. Further testing is required regarding whether the genes responsible for radical scavenger proteins are substantially upregulated in cultured T lymphocytes, and whether there are differences in levels of these proteins in cultured T lymphocytes from different individuals.

Differences in individual radiosensitivity were not as obvious in T lymphocytes cultured for 13 days (Fig. 4). Previously, it had been shown that the cell growth rate declined appreciably in similar T-cell cultures 10–14 days after the beginning of culture [Ishioka et al., 1997]. This decline may have been simply due to growth arrest mediated by attenuated T-cell receptor and/or growth factor signals. Simply stated, the diminished responses were probably the result of the cultured T lymphocytes being in a resting state at the time of testing (13th day).

γH2AX levels detected with FCM in a given fraction of irradiated T lymphocytes were able to fully reflect the mean number of microscopically detected γH2AX foci per cell in the same fraction (Fig. 6). It is probable that the γH2AX detected by FCM was related to the levels of radiation-induced DSBs in the same fraction as well. It is therefore likely that individual differences observed in γH2AX-FCM are related to differences in the degree of DNA damage and in the individual's ability to repair DNA damage.

In this study, there was no obvious difference in radiation-induced γH2AX levels between CD4 and CD8 T-cell populations obtained and cultured from the same individuals. Our previous study [Nakamura et al., 1990] showed that survival fractions after in vitro irradiation did not differ significantly between these subsets when they were isolated from the same individuals and irradiated before

culture with PHA and IL-2. Radiation-induced micronucleus frequencies also were similar among peripheral T-cell subpopulations [Ban and Cologne, 1992]. Therefore, it is likely that CD4 and CD8 T lymphocytes, which comprise the majority of peripheral blood T lymphocytes, exhibit comparable radiation sensitivities independent of their activation. Moreover, the cultured T-lymphocyte populations used in the present study for individual radiation sensitivity appeared to be mainly composed of memory T-lymphocytes, with more than half memory CD8 T-lymphocytes. It has been reported that memory T-lymphocytes are more radiation-sensitive than naïve T lymphocytes [Uzawa et al., 1994]. Therefore, it is possible that excessive proliferation of memory CD8 T-lymphocytes in the culture might affect the individual radiosensitivity difference that we detected with γH2AX-FCM. However, it is unlikely that the differences in the percentages of memory CD8 T-lymphocytes in the tested cell samples were related to the individual variability in radiation-induced γH2AX levels (data not shown). Accordingly, we believe that these relatively small differences in the proportion of T-lymphocyte subpopulations do not significantly influence the γH2AX-FCM testing procedures that we described for evaluating radiation sensitivity in vitro.

ACKNOWLEDGMENTS

The authors are grateful to Drs. Tomonori Hayashi, Seishi Kyoizumi, Asao Noda, Charles A. Waldren, and Thomas M. Seed for their helpful advice. They also would like to thank Mika Yamaoka and Yoshiko Kubo for their excellent assistance regarding the use of FCM.

The Radiation Effects Research Foundation (RERF), Hiroshima and Nagasaki, is a private nonprofit foundation funded by the Japanese Ministry of Health, Labour and Welfare, and the United States Department of Energy, the latter through the National Academy of Sciences. This publication was based on RERF Research Protocol RP 3-87.

REFERENCES

Ban S, Cologne JB. 1992. X-ray induction of micronuclei in human lymphocyte subpopulations differentiated by immunoperoxidase staining. Radiat Res 131:60–65.

Banath JP, Macphail SH, Olive PL. 2004. Radiation sensitivity, H2AX phosphorylation, and kinetics of repair of DNA strand breaks in irradiated cervical cancer cell lines. Cancer Res 64:7144–7149.

Celeste A, Petersen S, Romanienko PJ, Fernandez-Capetillo O, Chen HT, Sedelnikova OA, Reina-San-Martin B, Coppola V, Meffre E, Difilippantonio MJ, Redon C, Pilch DR, Olaru A, Eckhaus M, Camerini-Otero RD, Tessarollo L, Livak F, Manova K, Bonner WM, Nussenzweig MC, Nussenzweig A. 2002. Genomic instability in mice lacking histone H2AX. Science 296:922–927.

Celeste A, Fernandez-Capetillo O, Kruhlak MJ, Pilch DR, Staudt DW, Lee A, Bonner RF, Bonner WM, Nussenzweig A. 2003. Histone H2AX phosphorylation is dispensable for the initial recognition of DNA breaks. Nat Cell Biol 5:675–679.

Hagmar L, Stromberg U, Bonassi S, Hansteen IL, Knudsen LE, Lindholm C, Norppa H. 2004. Impact of types of lymphocyte chromosomal aberrations on human cancer risk: Results from Nordic and Italian cohorts. Cancer Res 64:2258–2263.

Ichijima Y, Sakasai R, Okita N, Asahina K, Mizutani S, Teraoka H. 2005. Phosphorylation of histone H2AX at M phase in human cells without DNA damage response. Biochem Biophys Res Commun 336:807–812.

Ishioka N, Umeki S, Hirai Y, Akiyama M, Kodama T, Ohama K, Kyoizumi S. 1997. Stimulated rapid expression in vitro for early detection of in vivo T-cell receptor mutations induced by radiation exposure. Mutat Res 390:269–282.

Kobayashi J. 2004. Molecular mechanism of the recruitment of NBS1/hMRE11/hRAD50 complex to DNA double-strand breaks: NBS1 binds to γ-H2AX through FHA/BRCT domain. J Radiat Res (Tokyo) 45:473–478.

Kushiro J, Hirai Y, Kusunoki Y, Kyoizumi S, Kodama Y, Wakisaka A, Jeffreys A, Cologne JB, Dohi K, Nakamura N, Akiyama M. 1992. Development of a flow-cytometric HLA-A locus mutation assay for human peripheral blood lymphocytes. Mutat Res 272:17–29.

Kusunoki Y, Kodama Y, Hirai Y, Kyoizumi S, Nakamura N, Akiyama M. 1995. Cytogenetic and immunologic identification of clonal expansion of stem cells into T,B lymphocytes in one atomic-bomb survivor. Blood 86:2106–2112.

Kusunoki Y, Kyoizumi S, Hirai Y, Suzuki T, Nakashima E, Kodama K, Seyama T. 1998. Flow cytometry measurements of subsets of T,B and NK cells in peripheral blood lymphocytes of atomic bomb survivors. Radiat Res 150:227–236.

Lavin MF, Kidson C. 1977. Repair of ionizing radiation induced DNA damage in human lymphocytes. Nucleic Acids Res 4:4015–4022.

MacPhail SH, Banath JP, Yu TY, Chu EH, Lambur H, Olive PL. 2003a. Expression of phosphorylated histone H2AX in cultured cell lines following exposure to X-rays. Int J Radiat Biol 79:351–358.

MacPhail SH, Banath JP, Yu Y, Chu E, Olive PL. 2003b. Cell cycle-dependent expression of phosphorylated histone H2AX: Reduced expression in unirradiated but not X-irradiated G1-phase cells. Radiat Res 159:759–767.

Mayer C, Popanda O, Zelezny O, von Brevern MC, Bach A, Bartsch H, Schmezer P. 2002. DNA repair capacity after γ-irradiation and expression profiles of DNA repair genes in resting and proliferating human peripheral blood lymphocytes. DNA Repair (Amst) 1:237–250.

McManus KJ, Hendzel MJ. 2005. ATM-dependent DNA damage-independent mitotic phosphorylation of H2AX in normally growing mammalian cells. Mol Biol Cell 16:5013–5025.

Mukherjee B, Kessinger C, Kobayashi J, Chen BP, Chen DJ, Chatterjee A, Burma S. 2006. DNA-PK phosphorylates histone H2AX during apoptotic DNA fragmentation in mammalian cells. DNA Repair (Amst) 5:575–590.

Nakamura N, Kusunoki Y, Akiyama M. 1990. Radiosensitivity of CD4 or CD8 positive human T-lymphocytes by an in vitro colony formation assay. Radiat Res 123:224–227.

Ohara M, Hayashi T, Kusunoki Y, Miyauchi M, Takata T, Sugai M. 2004. Caspase-2 and caspase-7 are involved in cytolethal distending toxin-induced apoptosis in Jurkat and MOLT-4 T-cell lines. Infect Immun 72:871–879.

Parshad R, Price FM, Bohr VA, Cowans KH, Zujewski JA, Sanford KK. 1996. Deficient DNA repair capacity, a predisposing factor in breast cancer. Br J Cancer 74:1–5.

Paull TT, Rogakou EP, Yamazaki V, Kirchgessner CU, Gellert M, Bonner WM. 2000. A critical role for histone H2AX in recruitment of repair factors to nuclear foci after DNA damage. Curr Biol 10:886–895.

Roberts SA, Spreadborough AR, Bulman B, Barber JB, Evans DG, Scott D. 1999. Heritability of cellular radiosensitivity: A marker of low-penetrance predisposition genes in breast cancer? Am J Hum Genet 65:784–794.

Rogakou EP, Pilch DR, Orr AH, Ivanova VS, Bonner WM. 1998. DNA double-stranded breaks induce histone H2AX phosphorylation on serine 139. J Biol Chem 273:5858–5868.

Rogakou EP, Boon C, Redon C, Bonner WM. 1999. Megabase chromatin domains involved in DNA double-strand breaks in vivo. J Cell Biol 146:905–916.

Scott D, Barber JB, Levine EL, Burrill W, Roberts SA. 1998. Radiation-induced micronucleus induction in lymphocytes identifies a high frequency of radiosensitive cases among breast cancer patients: A test for predisposition? Br J Cancer 77:614–620.

Scott D, Barber JB, Spreadborough AR, Burrill W, Roberts SA. 1999. Increased chromosomal radiosensitivity in breast cancer patients: A comparison of two assays. Int J Radiat Biol 75: 1–10.

Takahashi A, Ohnishi T. 2005. Does γH2AX foci formation depend on the presence of DNA double strand breaks? Cancer Lett 229: 171–179.

Terzoudi GI, Jung T, Hain J, Vrouvas J, Margaritis K, Donta-Bakoyianni C, Makropoulos V, Angelakis P, Pantelias GE. 2000. Increased G2 chromosomal radiosensitivity in cancer patients: The role of cdk1/cyclin-B activity level in the mechanisms involved. Int J Radiat Biol 76:607–615.

Uzawa A, Suzuki G, Nakata Y, Akashi M, Ohyama H, Akanuma A. 1994. Radiosensitivity of CD45RO+ memory and CD45RO− naive T cells in culture. Radiat Res 137:25–33.

West CM, Davidson SE, Elyan SA, Valentine H, Roberts SA, Swindell R, Hunter RD. 2001. Lymphocyte radiosensitivity is a significant prognostic factor for morbidity in carcinoma of the cervix. Int J Radiat Oncol Biol Phys 51:10–15.

Accepted by—
W. F. Morgan

RADIATION RESEARCH 166, 360–366 (2006)
0033-7587/06 $15.00

Levels of Antibodies to Microorganisms Implicated in Atherosclerosis and of C-Reactive Protein among Atomic Bomb Survivors

Masayuki Hakoda,[a,1] Fumiyoshi Kasagi,[b] Yoichiro Kusunoki,[c] Shinsuke Matsuura,[a] Tomonori Hayashi,[c] Seishi Kyoizumi,[c,2] Masazumi Akahoshi,[d] Gen Suzuki,[a] Kazunori Kodama[b] and Saeko Fujiwara[a]

Departments of [a] Clinical Studies, [b] Epidemiology and [c] Radiobiology/Molecular Epidemiology, Radiation Effects Research Foundation, Hiroshima, Japan; and [d] Department of Clinical Studies, Radiation Effects Research Foundation, Nagasaki, Japan

Hakoda, M., Kasagi, F., Kusunoki, Y., Matsuura, S., Hayashi, T., Kyoizumi, S., Akahoshi, M., Suzuki, G., Kodama, K. and Fujiwara, S. Levels of Antibodies to Microorganisms Implicated in Atherosclerosis and of C-Reactive Protein among Atomic Bomb Survivors. *Radiat. Res.* 166, 360–366 (2006).

Although it has been suggested that cardiovascular disease incidence is increased among atomic bomb survivors, the existence of a causal relationship between radiation exposure and atherosclerosis is unclear. Microbial infections, including those caused by *Chlamydia pneumoniae*, *Helicobacter pylori* and cytomegalovirus, have recently been implicated in atherosclerosis. Since immune function is somewhat impaired among atomic bomb survivors, their immune defense against such infections might be diminished. To investigate this possibility, we measured antibody levels to the above microorganisms in the sera of survivors. We found that the levels of IgG and IgA antibodies to *Chlamydia pneumoniae* decreased significantly with radiation dose, whereas the levels of IgG antibodies to *Helicobacter pylori* or cytomegalovirus remained unchanged. The inflammation marker C-reactive protein was significantly and positively associated with level of antibodies to *Chlamydia pneumoniae* only in heavily exposed (≥1000 mGy) survivors. These results may suggest that among atomic bomb survivors, immune response to *Chlamydia pneumoniae* is diminished and chronic inflammatory reactions related to *Chlamydia pneumoniae* infection are present. © 2006 by Radiation Research Society

INTRODUCTION

Mortality and incidence studies have suggested that cardiovascular disease is increased with radiation dose among atomic bomb (A-bomb) survivors (*1–3*). Long-term investigation of patients treated with radiation therapy for Hodgkin's lymphoma confirmed earlier observations that the treatment may have induced coronary heart disease (*4, 5*). The total local dose received by such patients, however, was about 30 Gy, whereas for A-bomb survivors, the total dose typically did not exceed 3 Gy (*6*). The possibility exists, therefore, that the mechanism for development of cardiovascular disease in A-bomb survivors differs from that in radiation therapy patients.

Although various factors initiate the atherosclerotic process, of which coronary heart disease is a typical clinical expression, inflammation accompanying activation of macrophages and T lymphocytes plays a central role (*7, 8*). The causal mechanism for development of this inflammatory process is not fully understood, but infectious agents have been implicated repeatedly (*9–12*). Among several pathogens, *Chlamydia pneumoniae*, *Helicobacter pylori* and cytomegalovirus have been investigated extensively, with *Chlamydia pneumoniae* regarded as the most plausible cause for the pathogenesis of atherosclerosis (*9–12*). Since impairment of immune function, especially decreased T-lymphocyte function, is suggested for A-bomb survivors (*13–16*), infectious agents may provide a plausible explanation for the development of atherosclerotic disease among this population.

It has been reported that mortality due to pneumonia is increased with radiation dose (*1*) and that this may be a reflection of increased infections among A-bomb survivors. Another example of increased infections among the survivors is the increase in the prevalence of hepatitis B virus surface antigen with radiation dose (*17–19*). On the other hand, tuberculosis mortality is not increased among A-bomb survivors (*1*). To further investigate infectious agents implicated in atherosclerosis among A-bomb survivors, we measured serum levels of antibodies to *Chlamydia pneumoniae*, *Helicobacter pylori* and cytomegalovirus in this survivor population and evaluated the association of the antibodies with radiation dose.

MATERIALS AND METHODS

Study Subjects

The study population comprised Adult Health Study (AHS) participants who had undergone biennial clinical examinations since 1958 at

[1] Address for correspondence: Department of Clinical Studies, Radiation Effects Research Foundation, 5-2 Hijiyama Park, Minami-ku, Hiroshima 732-0815, Japan; e-mail: hakoda@rerf.or.jp.

[2] Present address: Department of Nutritional Sciences, Faculty of Human Ecology, Yasuda Women's University, 13-1 Yasuhigashi 6-chome, Asaminami-ku, Hiroshima 731-0153, Japan.

the Radiation Effects Research Foundation (RERF) in Hiroshima and Nagasaki. The AHS was initiated to evaluate the long-term effects of ionizing radiation from the atomic bombs on human health (*20*). The original AHS cohort consisted of 19,961 individuals, approximately half of whom were exposed to the bombs proximally (<2,000 m from the hypocenter), with the other half exposed either distally (≥3000 m from the hypocenter) or not in the cities at the time of the bombings. The latter group of survivors was thus not exposed to substantial levels of A-bomb radiation. The design of the AHS has been described elsewhere (*20*). In 1977, 1,218 individuals whose estimated radiation dose was greater than 1 Gy, and the same number of controls distally exposed to the bomb, were newly added to the cohort. The 5,000 people who were not in the two cities at the time of the bombings were excluded from the AHS cohort in 1986. Thus there were 17,397 cohort members at that time. When this study began in March 2000, 10,030 cohort members had died and 1,058 had moved away from the two cities, so there were 6,309 AHS cohort members who were potentially able to visit the RERF clinic.

While almost 4,187 (66%) of the eligible cohort members agreed to visit RERF and undergo health examinations, 119 (3%) of these people did not consent to the antibody measurements for this study. Radiation dose estimates (DS86 whole-body kerma estimates) (*21*) were available for 3,476 (85%) of the 4,068 participants with antibody measurements. We obtained written informed consent from the subjects and approval from the institutional Human Investigation Committee. Body weight and height were measured during the participant's clinic visit. Body mass index (BMI) was calculated by dividing weight in kilograms by the square of height in meters. Smoking information (number of cigarettes smoked per day) was obtained through interview by nurses at the visit.

Laboratory Methods

Serum samples were obtained from each participant at the time of the clinic visit. Serum was stored at −80°C until use. Frozen serum samples obtained in Nagasaki were sent to Hiroshima for analysis. We used enzyme-linked immunosorbent assay (ELISA) kits to determine serum antibody levels. IgG and IgA antibodies to *Chlamydia pneumoniae* were measured using HITAZYME® *C. pneumoniae* Ab-IgG (Hitachi Chemical Co., Ltd., Tokyo, Japan) and HITAZYME® *C. pneumoniae* Ab-IgA (Hitachi Chemical Co., Ltd.), respectively. For IgG antibody to cytomegalovirus, we used CYTOMEGALO IgG (II)-EIA "SEIKEN" (DENKA SEIKEN Co., Ltd., Osaka, Japan), and for IgG antibody to *Helicobacter pylori*, we employed AUTOACE H. PYLORI G (AZWELL Inc., Osaka, Japan). Using these ELISA kits, we measured antibody levels in serum semi-quantitatively based on a comparison of optical density of the serum samples with that of the standard materials provided in the kits. The values obtained were expressed as units (U). In addition to sequential antibody levels, we used antibody status (positive or negative) for analysis. Following the manufacturers' instructions, we scored antibody level as positive if it measured ≥1.1 U for IgG or IgA antibody to *Chlamydia pneumoniae*, ≥16.5 U for IgG antibody to *Helicobacter pylori*, and ≥4 U for IgG antibody to cytomegalovirus.

We measured serum level of C-reactive protein (CRP), a sensitive marker for inflammation, using a validated, high-sensitivity assay kit (Nissui Pharmaceutical Co. Ltd., Tokyo, Japan) and an auto-analyzer (Clinical Analyzer 7170, Hitachi, Ltd., Tokyo, Japan), a robotic system used for the assay of many routine clinical biochemical parameters.

Statistical Analysis

The relationship between measurements of antibody levels (*response*) and radiation dose (*dose*) was analyzed by a multiple regression model, with adjustment for city, gender, age and smoking history, as follows:

$$\log(response) = \alpha + \beta_1 city + \beta_2 gender + \beta_3(age - 70) + \beta_4 smoking + \beta_5 dose,$$

where *city* = 0 for Hiroshima subjects, 1 for Nagasaki subjects; *gender* = 0 for males, 1 for females; *smoking* = number of cigarettes smoked per day; *dose* = exposed dose. Logarithmic transformation was applied to the dependent variable *response* to obtain a more normal distribution of antibody level. With this model, for any of the values of *city, gender, age* and *dose,* the increased rate of *response* per gray was calculated as e^{β_5} and its percentage change was $100(e^{\beta_5} - 1)$. The antibody levels for nonexposed nonsmoking males aged 70 years in Hiroshima were estimated by e^{α}.

For analysis of the relationship between antibody level and log-transformed CRP level, BMI centered at 23 kg/m² was included in the regression model as follows:

$$\log(CRP) = \alpha + \beta_1 city + \beta_2 gender + \beta_3(age - 70) + \beta_4 smoking + \beta_5(BMI - 23) + \beta_6 dose + \beta_7 response$$

The interaction between radiation dose and antibody level was tested by adding the term *dose* × *response* to the above model.

When the relationship was examined by dose category (0, 1–999 mSv, and ≥1000 mSv), the following model was applied:

$$\log(CRP) = \alpha + \beta_1 city + \beta_2 gender + \beta_3(age - 70) + \beta_4 smoking + \beta_5(BMI - 23) + \beta_6 response + \beta_7 d_1 \times response + \beta_8 d_2 \times response,$$

where $d_1 = 1$ for the 1–999-mGy group, = 0 otherwise; $d_2 = 1$ for the ≥1000-mGy group, = 0 otherwise. Accordingly, for any of the values of *city, gender, age* and *BMI,* the percentage change in *CRP* for 1 U of antibody level was estimated as $100(e^{\beta_6 \times unit} - 1)$ for 0 mGy, $100(e^{(\beta_6+\beta_7)\times unit} - 1)$ for 1–999 mGy, and $100(e^{(\beta_6+\beta_8)\times unit} - 1)$ for ≥1000 mGy. Heterogeneity among dose categories in the relationship between CRP and antibody level was tested by the null hypothesis, H_0: $d_1 = d_2 = 0$.

For the dichotomous summaries (positive or negative) of antibody measurements, binominal odds regression model was used to analyze relationship with radiation dose, and adjustment was made for age, gender and smoking history.

RESULTS

Table 1 shows the number of individuals in each radiation dose category and the mean and median serum levels of antibodies to *Chlamydia pneumoniae*, *Helicobacter pylori* and cytomegalovirus. The antibody level to cytomegalovirus was not measured for the subjects who came to RERF after about the halfway point of this study (14 months after the start of the study). Thus the antibody level to cytomegalovirus was measured for 2,049 subjects but was not for the rest of the subjects. This was because the proportion of subjects who had a positive response to cytomegalovirus was very high (more than 99%) among those whose antibody level had been measured before that time. A high prevalence of positive IgG antibody response to cytomegalovirus was also reported in a different region of Japan (*22*).

Table 2 shows the association of the level of IgG antibody to *Chlamydia pneumoniae* with radiation dose. Since antibody level was significantly associated with male gender, older age, and cigarette smoking, we adjusted for those factors in addition to city in the multivariate regression analysis. After the adjustments, the serum level of IgG an-